

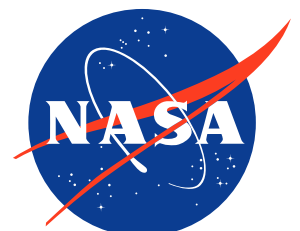


Commercial Satellite Data Acquisition Program

Capella Space Radiometric & Geo- metric Quality Assessment Report



Goddard Space Flight Center
Greenbelt, MD



Commercial Satellite Data Acquisition Program Capella Space Radiometric & Geometric Quality Assessment Report

Signature/Approval Page

Approval by:

Melissa Yang Martin
Commercial Satellite Data Acquisition Program Manager
Earth Science Division
Headquarters/NASA

Date

Accepted by:

Dana Ostrenga
Commercial Satellite Data Acquisition Project Manager
Earth Science Division
GSFC /NASA

Date

Preface

This document is under CSDA Project configuration control. Once this document is approved, CSDA approved changes are handled in accordance with Class I and Class II change control requirements described in the CSDA Configuration Management Procedures based on NASA standard configuration practices, and changes to this document shall be made by document change notice (DCN), documented in the Change History Log or by complete revision.

Abstract

The evaluation summarized in this report was conducted by subject matter experts (SMEs) funded by NASA's Commercial Satellite Data Acquisition (CSDA) Program. The SMEs evaluated the radiometric and geometric quality of Capella Space data for the NASA Earth science research and applications community. The results of the evaluation help to inform NASA program management on the quality of the data for NASA science.

Cover Art: Cover art is AI generated graphic using Microsoft Copilot Designer using term "commercial satellite constellation Earth observation across Atlantic AND Northern Hemisphere AND digital downlink"

Authored and prepared by

Batuhan Osmanoglu

CSDA SAR Subject Matter Expert
National Aeronautics and Space Administration

Dylan Boyd

SAR Evaluation Assistant
University of Maryland, College Park
National Aeronautics and Space Administration

Jordan Bell

CSDA SAR Subject Matter Expert
National Aeronautics and Space Administration

MinJeong Jo

SAR Quality Assessment Expert
University of Maryland, Baltimore County
National Aeronautics and Space Administration

Jaime Nickeson

CSDA Technical Science Coordinator
Science Systems and Applications Inc
National Aeronautics and Space Administration

Frederick Policelli

CSDA Project Scientist
National Aeronautics and Space Administration

Change History Log

Revision	Effective Date	Description of Changes
1.0	6/23/2025	First reviewed version for public release

Table of Contents

Executive Summary	9
1 Cal/Val Maturity Matrices	11
1.1 Summary Cal/Val Maturity Matrix	11
1.2 Detailed Validation Maturity Matrix.....	12
2 Data Provider Documentation Review.....	13
2.1 Product Information.....	13
2.2 Metrology.....	16
2.3 Product Generation	18
3 Detailed Validation – Radiometric	19
3.1 Absolute Radiometric Calibration	20
3.1.1 Method	20
3.1.2 Results Compliance	20
3.2 Radiometric Stability	21
3.2.1 Method	21
3.2.2 Results Compliance	21
3.3 Sensitivity Validation	22
3.3.1 Method	22
3.3.2 Results Compliance	22
3.4 Polarimetric Accuracy.....	23
3.4.1 Method	23
3.5 Interferometric Accuracy	23
3.5.1 Method	23
4 Detailed Validation – Geometric.....	23
4.1 Spatial Resolution	28
4.1.1 Method	28
4.1.2 Results Compliance	29
4.2 Geolocation Accuracy	36
4.2.1 Method	36
4.2.2 Results Compliance	37
5 References.....	41
APPENDIX A	42

List of Figures

Figure 1. Summary Cal/Val Maturity Matrix for Capella Space	11
Figure 2. Detailed Validation Maturity Matrix for the SAR domain	12
Figure 3. Sigma0 values observed across the swath over various sites in Amazon.....	20
Figure 4. Sensitivity of Capella constellation observed over the Doldrums.....	23
Figure 5. The upper image is a Google Earth overview of the Rosamond site.	25
Figure 6. A Google Earth view of the NISAR Calibration array in Oklahoma.	27
Figure 7. Google Earth view of the OPERA calibration stations in California.	28
Figure 8. Example of point target analysis using GAMMA ptarg_SLC module.	29
Figure 9. Simulated impulse response using Avci-Nacaroglu and Rectangular windowing	30
Figure 10. Point target showing abnormal focusing in range direction	33
Figure 11. Point target showing a double peak in azimuth direction.....	34
Figure 12. Geolocation accuracy assessment with GAMMA software.	36
Figure 13. Geolocation errors of Capella SM, SP, and SS mode images.	39

List of Tables

Table 1. Summarized list of Capella Space data used for the radiometric assessment.....	19
Table 2. Radiometric Stability results over Rosamond corner reflectors.	21
Table 3. Summarized list of Capella Space data used for the IRF assessment.....	24
Table 4. Corner Reflectors used for the analysis at the Rosamond site.....	25
Table 5. Corner Reflectors used for the analysis at the Oklahoma site.	27
Table 6. Corner Reflectors used for the analysis at the OPERA calibration site.	28
Table 7. Specification of the standard single look complex (SLC) image product type	29
Table 8. Simulated PSLR and ISLR values based on windowing parameters.	30
Table 9. Observed spatial resolution, PSLR and ISLR values over Rosamond, CA.....	31
Table 10. Observed spatial resolution, PSLR and ISLR values over Oklahoma.....	34
Table 11. The IRF analysis for the OPERA Calibration site.....	35
Table 12. Rosamond geolocation accuracy analysis for Capella Space	37
Table 13. Geolocation accuracy analysis over the Oklahoma site.....	39
Table 14. Geolocation accuracy analysis over the OPERA calibration site.	40
Table A1. Capella Space data products used for the assessment.	42
Table A2. List of Capella acquisitions used for the IRF assessment.	43

Acronyms & Abbreviations

ALE	Absolute Location Error
CPHD	Compensated Phase History Data
CR	Corner Reflector
CSDA	Commercial Satellite Data Acquisition
EDAP	Earthnet Data Assessment Pilot
ESA	European Space Agency
EULA	End User License Agreement
FAIR	Findable, Accessible, Interoperable, Reusable
GEC	Geocoded Ellipsoid Corrected
GEO	Geocoded Terrain Corrected
GeoTIFF	Geographic Tag Image File Format
GSFC	Goddard Space Flight Center
HH	Horizontal-Horizontal (polarization)
IRF	Impulse Response Function
InSAR	Interferometric SAR
ISCE	InSAR Scientific Computing Environment
ISLR	Integrated Side-Lobe Ratio
ISRO	Indian Space Research Organization
JPL	Jet Propulsion Laboratory
JSON	JavaScript Object Notation
MERRA-2	Modern-Era Retrospective Analysis for Research and Applications, V.2
N/A	Not Applicable / Not Available
NASA	National Aeronautics and Space Administration
NEBN	Noise Equivalent Beta Nought
NESZ	Noise Equivalent Sigma Zero
NISAR	NASA-ISRO SAR
NOTA	Network of the Americas
OPERA	Observational Products for End-Users from Remote Sensing Analysis
PSLR	Peak Side-Lobe Ratio
RCRA	Rosamond Corner Reflector Array
SAR	Synthetic Aperture Radar
SICD	Sensor Independent Complex Data
SIDD	Sensor Independent Derived Data
SP	Spotlight
SS	Sliding Spotlight
SLC	Single-Look Complex
SM	Stripmap
SNAP	Sentinel Application Platform
VV	Vertical-Vertical (polarization)
WGS84	World Geodetic System 1984
XML	Extensible Markup Language

Executive Summary

The Commercial Satellite Data Acquisition (CSDA) Program was established to identify, evaluate, and acquire data from commercial sources that support the National Aeronautics and Space Administration (NASA) Earth science research and application goals. NASA's Earth Science Division (ESD) recognizes the potential impact commercial satellite constellations may have in encouraging/enabling efficient approaches to advancing Earth System Science and applications development for societal benefit. Commercially acquired data may also provide a cost-effective means to augment and/or complement the suite of Earth observations acquired by NASA and other U.S. government agencies and those by international partners and agencies.

In this report, CSDA provides an evaluation of the quality of data provided by the Capella Space (at times referred to as Capella) X-band Synthetic Aperture Radar (SAR) satellite constellation for advancing NASA's Earth system science research and applications. This evaluation of Capella Space radiometric and geometric performance was carried out by NASA subject matter experts (SMEs) that were enlisted to evaluate the fundamental quality of the Capella Space data following the Joint NASA/European Space Agency (ESA) assessment guidelines (ESA-NASA, 2024).

Data from the Capella Space constellation of satellites C2-C14 were analyzed including archive data from satellites that were no longer operational during the evaluation period. All data products were version 1.10 and were processed using software versions 2.44.1 to 2.57.2. Details about an assessment performed by a group of selected principal investigators on the utility of Capella Space data for NASA science is available in a separate report, the *Commercial Satellite Data Acquisition Program Capella Space Principal Investigator Evaluation Report*.

Only the documents provided by Capella Space for the evaluation were considered as part of the assessment. Additional documentation with more detailed description of the calibration and validation procedures may be available online, but any document that is not listed in this report was not considered in the evaluation. The product information provided in the vendor documentation and the product metadata together provided adequate information to work with the data. The product details in the metadata were provided in the common JavaScript Object Notation (JSON) file format. These documents provide a characterization of the SAR system and data, together with the metadata, that include relevant ancillary information. Documentation provided to CSDA included limited pre- and post-flight calibration information. Metrological traceability documentation was not provided to CSDA.

The quality assessment was mainly performed on the single look complex (SLC) Level 1 data products. Additional Level 2 products were also used in science usability assessments by the evaluation team. The uncertainty values relevant for SAR (i.e. noise equivalent sigma naught [NESZ]) are provided at the product level in the metadata. A "scale_factor" for each product is provided in the metadata to convert the observed radar brightness to meaningful units (i.e. σ_0). Expected and observed values for relevant metrics such as absolute radiometric accuracy, relative radiometric accuracy, NESZ, peak sidelobe ratio (PSLR), and integrated sidelobe ratio (ISLR) are discussed within the results compliance sections of this document. The vendor provided documentation does not contain information on how the performance values are obtained.

An independent quality assessment of the essential quality parameters of SAR, such as spatial resolution, PSLR, ISLR, NESZ, absolute and relative radiometric accuracy was performed by the CSDA team. Representative datasets collected by Capella Space over various test sites, including distributed and point targets were used. Data from Spotlight (SP), Sliding Spotlight (SS), and Stripmap (SM) modes were analyzed. The validation by the CSDA Program was performed using multiple software packages, including code developed internally at NASA Goddard Space Flight Center (GSFC), the GAMMA Remote Sensing commercial processing package, and ESA's Sentinel Application Platform (SNAP) architecture. In addition to these software packages, the PI teams also processed the data using JPL's InSAR (interferometric SAR) Scientific Computing Environment (ISCE). The quality analysis results were generally in agreement with the values provided by Capella Space, such as the spatial resolution and geolocation accuracy. The measured PSLR values were generally close to the expected theoretical values. Based on the available Capella Space documentation and our independent data analysis, we conclude that the Capella Space data are of good quality.

1 Cal/Val Maturity Matrices

1.1 Summary Cal/Val Maturity Matrix

Data Provider Documentation Review			Validation Summary	Key
Product Information	Metrology	Product Generation		Not Assessed
Product Details	Radiometric Calibration & Characterization	Radiometric Calibration Algorithm	Radiometric Validation Method	Not Assessable
Availability & Accessibility	Geometric Calibration & Characterization	Geometric Processing	Radiometric Validation Results Compliance	Basic
Product Format, Flags & Metadata	Metrological Traceability Documentation	Higher Level Retrieval Algorithm	Geometric Validation Method	Good
User Documentation	Uncertainty Characterization	Mission Specific Processing	Geometric Validation Results Compliance	Excellent
	Ancillary Data			Ideal

🔒 Not Public

Figure 1. Summary Cal/Val Maturity Matrix for Capella Space

1.2 Detailed Validation Maturity Matrix

Validation Summary	Detailed Validation					
	Radiometric Validation Method	RADIOMETRIC	Absolute Radiometric Calibration	Radiometric Stability	Sensitivity Validation	Polarimetric Accuracy
Radiometric Validation Results Compliance	Absolute Radiometric Calibration Results Compliance		Radiometric Stability Results Compliance	Sensitivity Validation Results Compliance	Polarimetric Accuracy Results Compliance	Interferometric Accuracy Results Compliance
Geometric Validation Method	GEOMETRIC	Spatial Resolution	Geolocation Accuracy			
Geometric Validation Results Compliance		Spatial Resolution Results Compliance	Geolocation Accuracy Results Compliance			

Key
Not Assessed
Not Assessable
Basic
Good
Excellent
🔒 Not Public

Figure 2. Detailed Validation Maturity Matrix for the SAR domain, showing the Validation Summary column from the Summary Cal/Val Maturity Matrix.

2 Data Provider Documentation Review

2.1 Product Information

Product Details	
Grade: Good	
Justification	Robust description of products and associated metadata. Data such as temporal extent, spatial extent, and number of active satellites is not explicit in vendor-provided top-level documentation but can be determined through metadata catalog.
Product Name	<p>From the Capella Space SAR Products Format Specification (Capella Space, 2023), page 6: EEEEEEE_SSS_MM_PPP_HH_SSSSSSSSSSSSSSSSS_EEEEEEEEEEEEE EEE, where,</p> <ul style="list-style-type: none"> • EEE = Company Name (Capella) • SSS = Satellite ID (i.e., Capella-1 = C01, Capella-2=C02) • MM = acquisition mode (SP = Spotlight, *SS = Sliding Spotlight, SM = Stripmap) • HH = polarization (HH and VV polarization IDs) • SSSSSSSSSSSSSSSSS = acquisition start time (YYYYMMDDTHHMMSS) • EEEEEEEEEEEEEEEEE = acquisition end time (YYYYMMDDTHHMMSS) <p><i>Note that while the product format documentation (referenced above) provided to the evaluation team indicates that the Sliding Spotlight product file names are denoted with "SL", the actual file names of the Sliding Spotlight imagery received were denoted instead with "SS."</i></p>
Sensor Name	Capella Space SAR Series
Sensor Type	X-band (9.4 - 9.9 GHz) SAR
Mission Type	Monostatic SAR Constellation
Mission Orbit	Sun Synchronous (SSO) and Mid-Inclination Orbit (MIO)
Product Version Number	Product Version 1.10, Software Version 2.44.1 to 2.57.2
Product ID	A string of digits and letters (individual for each product) e.g. : "collect_id": "e0755b9e-0db2-4a4a-badf-c151eee21fe3"
Processing level of product	Level 1 (SLC imagery)
Measured Quantity Name	Radar backscatter, Beta Nought (β_0) (from the Capella Space SAR Products Format Specification (Capella Space, 2023) and product metadata
Measured Quantity Units	Radar backscatter (β_0) is a unitless quantity representing reflectivity per unit area.

Stated Measurement Quality	NESZ provided in the metadata.			
Spatial Resolution	From Table 5, 6, & 7 of the Capella Space SAR Imagery Products Guide (Capella Space, 2022)			
		Azimuth [m]	Slant Range [m]	Ground Range [m]
	Spotlight	0.5	0.3	0.5 – 0.7
	Sliding Spotlight	1.0	0.5	0.8 – 1.2
	Stripmap	1.2	0.75	1.1 – 1.6
Spatial Coverage		Range [km]	Azimuth [km]	
	Spotlight	5	5	
	Sliding Spotlight	5	10	
	Stripmap	5	20	
Temporal Resolution	Temporal resolution can be varied based on customer order. Combined satellites allow for sub-daily revisit time.			
Temporal Coverage	October 19th, 2020 – present			
Point of Contact	Brittany Ferrari, brittney.ferrari@capellaspace.com			
Product locator (DOI/URL)	N/A			
Conditions for access and use	All data used in this evaluation were purchased by CSDA under U.S. Government-wide license. Licenses can be found on the CSDA website (https://www.earthdata.nasa.gov/about/csda/commercial-datasets).			
Limitations on public access	N/A			
Product Abstract	N/A			

Availability & Accessibility	
Grade: Good	
Justification	Meets 14/17 of FAIR guiding principles. Unfulfilled principles are: F1: (Meta)data are assigned a globally unique and persistent identifier A2: Metadata are accessible, even when the data are no longer available I3: (Meta)data include qualified references to other (meta)data
Compliant with FAIR principles	82%
Data Management Plan	The vendor data management plan is described in (Capella Space, 2022)
Availability Status	Data are available to customers through a vendor provided API and web portal.

Product Format, Flags & Metadata									
Grade: Good									
Justification	Evaluated data is made available in folders containing 6 files: catalog metadata, image data, digest file, extended metadata, and a preview file. Metadata is provided in JSON format.								
Product File Format	<table border="1" style="width: 100%; border-collapse: collapse;"> <thead> <tr> <th style="text-align: center;">Format</th> <th style="text-align: center;">Associated Products</th> </tr> </thead> <tbody> <tr> <td>GeoTIFF + JSON</td> <td>Single-look complex (SLC), Geocoded ellipsoid corrected (GEC), Geocoded terrain corrected (GEO)</td> </tr> <tr> <td>NITF</td> <td>Sensor independent complex data (SIDC), Sensor independent derived data (SIDD)</td> </tr> <tr> <td>CPHD (binary data)</td> <td>Compensated phase history data</td> </tr> </tbody> </table>	Format	Associated Products	GeoTIFF + JSON	Single-look complex (SLC), Geocoded ellipsoid corrected (GEC), Geocoded terrain corrected (GEO)	NITF	Sensor independent complex data (SIDC), Sensor independent derived data (SIDD)	CPHD (binary data)	Compensated phase history data
Format	Associated Products								
GeoTIFF + JSON	Single-look complex (SLC), Geocoded ellipsoid corrected (GEC), Geocoded terrain corrected (GEO)								
NITF	Sensor independent complex data (SIDC), Sensor independent derived data (SIDD)								
CPHD (binary data)	Compensated phase history data								
Metadata Conventions	Product version 1.10								
Analysis Ready Data?	No								

User Documentation	
Grade: Good	
Justification	The user documentation and associated references provided to CSDA evaluators detail many aspects of product generation and the required auxiliary data. However, the documents do not provide traceable quality information for the provided uncertainty values.
Document	Reference
Product User Guide	<ul style="list-style-type: none"> • Capella Space SAR Imagery Products Guide (Capella Space, 2022) • Capella Space SAR Products Format Specification (Capella Space, 2023)
ATBD	Not available. Some details in the documentation files above.

2.2 Metrology

Radiometric Calibration & Characterization	
Grade: Good	
Justification	Vendor provides peak and range-dependent NESZ estimates within each metadata file. A vendor provided calibration coefficient is provided in the associated metadata. Explicit description of calibration and characterization is not available in documentation provided to evaluation team.
References	<ul style="list-style-type: none"> • Capella Space SAR Imagery Products Guide (Capella Space, 2022) • Capella Space SAR Products Format Specification (Capella Space, 2023)

Geometric Calibration & Characterization	
Grade: Good	
Justification	While geometric accuracy is acknowledged, vendor-provided geolocation accuracy and calibration is not present in documentation provided to assessment team.
References	<ul style="list-style-type: none"> • Capella Space SAR Imagery Products Guide (Capella Space, 2022) • Capella Space SAR Products Format Specification (Capella Space, 2023)

Metrological Traceability Documentation	
Grade: Not Assessable	
Justification	The evaluation team did not have access to metrological traceability documentation.
References	<ul style="list-style-type: none"> • Capella Space SAR Imagery Products Guide (Capella Space, 2022) • Capella Space SAR Products Format Specification (Capella Space, 2023)

Uncertainty Characterization	
Grade: Basic	
Justification	Limited descriptions of uncertainty are provided through estimates of NESZ. Vendor-provided data products do not appear to contain Guide to the Expression of Uncertainty in Measurement (GUM, JCGM 2008)-compliant uncertainty metrics.
References	<ul style="list-style-type: none"> • Capella Space SAR Imagery Products Guide (Capella Space, 2022) • Capella Space SAR Products Format Specification (Capella Space, 2023)

Ancillary Data	
Grade: Excellent	
Justification	Ancillary data used in product generation are specified and appear sufficient on a per-product basis. The ancillary metadata provided by the vendor, such as terrain models used in ground projection, are traceable and “fit for purpose” for the mission's stated performance.
References	<ul style="list-style-type: none"> • Capella Space SAR Products Format Specification (Capella Space, 2023)

2.3 Product Generation

Radiometric Calibration Algorithm	
Grade: Good	
Justification	SLC, GEC, and GEO image generation is detailed in the Capella documents below. The metadata provides a scale factor variable which serves as a calibration factor. Documentation references the option to generate imagery via back projection, omega-k, and range-Doppler algorithms. Detailed descriptions or references to the specific implementation are not present in vendor-provided documentation. Metadata contains image-dependent information such as the DEM used in GEO generation. The metadata provides a polynomial of the estimated NESZ to indicate the quality of the calibration. The metadata also describes the type of calibration and internal calibration ID used by the vendor.
References	<ul style="list-style-type: none"> • Capella Space SAR Imagery Products Guide (Capella Space, 2022) • Capella Space SAR Products Format Specification (Capella Space, 2023)

Geometric Processing	
Grade: Good	
Justification	Geometric processing is described in the Capella Space documentation, however with limited details. While Algorithm Theoretical Basis Document (ATBD)-level descriptions of the geometric processing approach are absent in vendor-provided documentation, the associated metadata for each product provides the explicit DEM and geocoding algorithm employed. The geocoding algorithms used are standard.
References	<ul style="list-style-type: none"> • Capella Space SAR Imagery Products Guide (Capella Space, 2022) • Capella Space SAR Products Format Specification (Capella Space, 2023)

Higher Level Retrieval Algorithm	
Grade: Not Assessable	
Justification	Higher-level data products are beyond the scope of this study. The primary service of this commercial constellation is on-demand SAR imagery with configurable resolution and scene extent. A dedicated higher-level data product is not currently associated with this constellation.
References	N/A

Mission Specific Processing	
Grade: Not Assessable	
Justification	This assessment is restricted to the provided SLC and ground-projected SAR data products. No additional evaluation of mission specific data products such as classification maps or deformation maps were performed in this evaluation.
References	N/A

3 Detailed Validation – Radiometric

This section presents the detailed measurement validation such as the absolute radiometric accuracy, radiometric stability, and sensitivity assessments conducted with Capella dataset. For the radiometric analyses the σ_0 was calculated using:

$$\sigma_{0dB} = 10 \log_{10} ((SC |DN_{SLC}|)^2 \sin(\theta))$$

where SC denotes scaling coefficient, DN_{SLC} is the dynamic number in the SLC product and θ is the incidence angle. In RD-2, this equation is given without the incidence angle term, but above equation is consistent with the ones used in ESA’s SNAP and the Gamma software package. This analysis includes data from the Capella Space constellation as shown in Table 1.

Table 1. Summarized list of Capella Space data used for the radiometric assessment. A detailed list of the parameters for individual satellite scenes used in the assessment is available in Appendix A, Table A1.

Test Area	Satellite Number	Imaging Mode	Polarization	Number of Scenes	Acquisition Date	Incidence Angle	Processor Version
Rosamond	C03, C05, C07, C08	SM	VV	20	03/27/2022 - 04/05/2023	28.4 - 47.9	2.21.1 - 2.38.5
Doldrums	C09, C10, C14	SM	HH	8	05/17/2024 - 06/09/2024	23.3 - 53.7	2.57.3 - 2.57.4
	C09, C10	SS	HH	2	05/27/2024 - 05/30/2024	35.1 - 45.9	2.57.4
	C09, C14	SS	VV	2	5/25/24	24.2 - 38.3	2.57.4
Amazon	C09, C10	SM	HH	6	05/20/2024 - 06/01/2024	25.0 - 54.9	2.57.3 - 2.57.4
	C09, C10	SM	VV	10	05/23/2024 - 05/28/2024	17.2 - 54.3	2.57.4
	C09, C10	SS	HH	5	05/26/2024 - 06/08/2024	19.9 - 43.6	2.57.4
	C09, C10, C14	SS	VV	10	05/24/2024 - 06/08/2024	26.4 - 53.2	2.57.4

3.1 Absolute Radiometric Calibration

3.1.1 Method

Absolute radiometric accuracy of the imagery was validated using both the Amazon rainforest and the Rosamond corner reflector array (RCRA), operated and maintained by JPL. The Amazon rainforest was used as a distributed target under the assumption that it represents a uniform and invariant target across the swath. This assumes that the σ_0 measurement uncertainty is zero (i.e., speckle is ignored). For a point target, such as the corner reflectors at Rosamond, the absolute radiometric accuracy measures the uncertainty in measurement of the radar cross section (RCS) considering an invariant and well-known ground target.

3.1.2 Results Compliance

The expected σ_0 value over a tree-covered surface in X-band HH and VV mode imagery for incidence angles between 16 and 55 degrees is about -10.9 dB for both polarizations. As shown in Figure 3, the calibrated Capella σ_0 values have a mean value of -8.0 dB and -5.2 dB for SS and SM imagery, or within about 2.9 to 5.7 dB of our expectation depending on the mode.

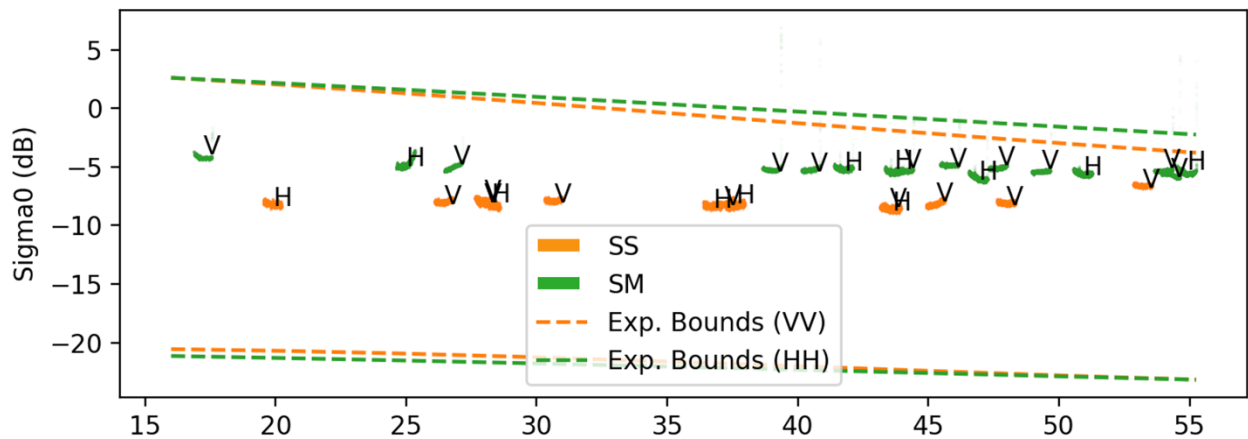


Figure 3. σ_0 values observed across the swath over various sites in Amazon indicate most of the scenes are calibrated well enough to fall within the expected range. SS and SM imagery are showing a difference in absolute calibration. The dashed green and orange lines mark the ± 3 -sigma values for the expected range of X-band VV and HH σ_0 values per Ulaby et al. (2019), respectively.

The RCRA array has 0.7 m, 2.4 m and 4.8 m corner reflectors. A set of 20 ascending, left looking, VV polarization images from the Capella C03, C05, C07, and C08 satellites were analyzed. The 0.7-m corner reflectors are most suitable for the high-resolution X-band sensors and have a mean absolute error of -2.4 dB. The 2.4 m and 4.8 m reflectors are better suited for L- and P-band sensors and show mean absolute errors of -14.9 and -18.6 dB, respectively (Table 2).

Table 2. Radiometric Stability results over Rosamond corner reflectors.

CR ID	Size (m)	Observed (dB)		Error (dB)	
		Mean	Std	Mean	Std
28	0.7	24.4	2.6	-5.2	2.1
31	0.7	25.1	2.1	-3.5	1.6
33	0.7	25.2	1.6	-2.4	1.8
34	0.7	25.3	1.5	-1.5	2.4
13	2.4384	38.4	3.9	-12.7	3.6
14	2.4384	24.3	5.4	-27.1	5.4
15	2.4384	34.0	5.1	-17.4	4.7
16	2.4384	34.5	4.0	-17.1	3.7
17	2.3989	39.8	5.7	-11.5	5.2
18	2.4384	31.1	4.9	-20.4	4.7
19	2.4384	39.0	4.6	-12.2	4.0
23	4.8	42.3	3.7	-18.6	3.1
24	4.8	42.9	4.0	-18.0	3.1
25	4.8	39.8	2.6	-21.1	3.1
26	4.8	43.2	2.9	-17.6	3.3
27	4.8	42.3	2.8	-18.5	2.9

3.2 Radiometric Stability

3.2.1 Method

Radiometric stability of the imagery was validated using the Amazon rainforest and RCRA. The Amazon rainforest was used as a distributed target under the assumption that it represents a uniform and invariant target across the swath, and that the temporal variation of the target area is minimal. The corner reflectors at RCRA were used as stable, well-defined targets. Radiometric stability was then calculated based on the repeated independent measurements of the reflectivity (σ_0) of this stable target. This target can be situated anywhere within the system dynamic range and swath, assuming that the uncertainty in measurement of the σ_0 is zero (i.e., speckle is ignored).

3.2.2 Results Compliance

The expected variation of σ_0 value over a tree covered surface at X-band for VV- and HH-polarizations and incidence angles between 16 and 55 degrees is about 3.4 dB and 3.7 dB respectively. As shown in Figure 3, the calibrated Capella σ_0 values have an overall standard deviation of 0.7 dB and 0.3 dB for SM and SS mode imagery, respectively. When both datasets are analyzed together, their standard deviation is around 1.7 dB.

Over the RCRA, there are 3 corner reflector sizes. The 0.7 m corner reflectors have a temporal variability of about 1.5-2.4 dB, while the 2.4 m and the 4.8 m corner reflectors have a temporal variability of 3.9-5.7 dB and 2.6-4.0 dB respectively (Table 2).

The stability observed over the Amazon rainforest was sufficiently stable, and the Rosamond site also exhibited overall variation below 5 dB. Therefore, the radiometric stability performance of the Capella imagery was assessed as good.

3.3 Sensitivity Validation

3.3.1 Method

NESZ is estimated using signal-free regions (e.g., over very low or null backscatter targets, such as calm water or deserts) in the radar imagery. For this analysis, we used imagery over the Doldrums. Near surface level (2 m above ellipsoid) wind conditions at the time of each acquisition were also observed through the closest surface-level wind estimate of the Modern-Era Retrospective Analysis for Research and Applications, Version 2 (MERRA-2) reanalysis (Gelaro et al., 2017) to ensure that the observations were on typically calm days (wind speed < 2 m/s). The expected σ_0 values were calculated using a geophysical model function. The XMOD2 (Li & Lehner, 2013) model was used for this analysis.

3.3.2 Results Compliance

Capella NESZ values are reported in each product metadata, and in most cases, they are around -18 dB. The actual values reported in the metadata are shown in Figure 4 with dashed lines. Figure 4 shows the observed σ_0 values for SM and SS products at varying incidence angles. The scenes used in this assessment are listed in Table 1.

In Figure 4, the solid red line denotes the expected σ_0 value given an assumption of 2 m/s wind speed. The analysis was bounded with windspeeds estimated close to the time of acquisition using MERRA-2 data, excluding any scene that was collected with windspeeds above 4 m/s. The average windspeed for the scenes included in the analysis were 3.2 m/s with a standard deviation of 1.0 m/s. The observed σ_0 values (colored dots) are very close to the expectation above a 40-degree incidence angle. For smaller incidence angles, it is possible that we are reaching the analysis limit and cannot retrieve the reported NESZ values, even in low-wind conditions.

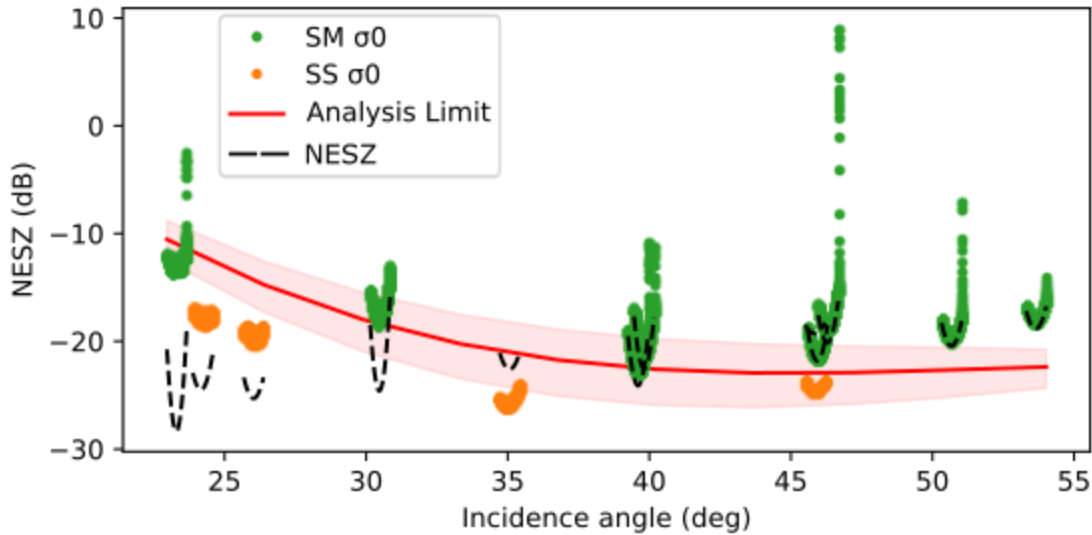


Figure 4. Sensitivity of Capella constellation observed over the Doldrums. Colored scattered plots depict observed sigma₀ values for different image modes. The black dashed lines indicate reported NESZ values in the metadata files. The solid red line indicates the XMOD2 calculated sigma₀ for a 2m/s wind-speed at Capella center frequency of 9.65GHz. The red shaded area indicates expected analysis limits. Starting around 35 degrees, we see that instrument performance (colored dots) is either at or below the expected NESZ. For angles less than 35 degrees, the NESZ is expected to be lower than the measurement due to analysis limits.

3.4 Polarimetric Accuracy

3.4.1 Method

Polarization accuracy can be measured using corner reflectors if quad polarization imagery is available (van Zyl, 1990). Capella imagery is limited to co-pol observations and can only collect HH or VV imagery at different times. Therefore, polarimetric accuracy was not evaluated.

3.5 Interferometric Accuracy

3.5.1 Method

The interferometric quality is assessed through tracking of point target phase over time for various targets across the image swath (Marinkovic et al., 2007). Repeat track Capella imagery was not available as a product during the time of the evaluation. Therefore, interferometric accuracy was not evaluated.

4 Detailed Validation – Geometric

This section describes detailed information of the impulse response function (IRF) quality assessment using point target analysis tools provided in GAMMA software, in terms of -3 dB width spatial resolution, Peak Sidelobe Ratio (PSLR), Integrated Sidelobe Ratio (ISLR), and geolocation accuracy. The test datasets were collected from various Capella satellites, including Stripmap (SM), Spotlight (SP), and Sliding Spotlight (SS) scenes as SLC product type. Table 1

lists the Capella scenes used for the IRF quality assessment, showing test areas, satellite numbers, imaging modes, polarization, acquisition dates, incidence angles, and processing versions of the product used by the vendor.

The IRF analysis was performed over dedicated calibration sites with installed trihedral corner reflectors (CRs). The calibration sites used in this study include the RCRA in Rosamond, CA, the Oklahoma Calibration Array in NASA-ISRO SAR (NISAR) Mission found in multiple cities across Oklahoma, and the Observational Products for End-users from Remote Sensing Analysis (OPERA) corner reflector installation in San Andreas, CA. For the Rosamond site, 33 SM, 5 SP, and 21 SS scenes were acquired. Additionally, 10 SM and 10 SS scenes were acquired for the Oklahoma site. For the OPERA Calibration and Validation (Cal/Val) site, 12 SM and 6 SS were collected for the analysis.

Most of Capella’s Spotlight products were processed using the Polar Format Algorithm (PFA) and were not compatible with the analysis tools available to CSDA. Therefore, only five Spotlight scenes for the Rosamond site that were focused with back-projection algorithm (BPA), were used in the analysis below.

Table 3. Summarized list of Capella Space data used for the IRF assessment. A detailed list of the parameters for individual satellite scenes used in the assessment is available in Appendix A, Table A2.

Test Area	Satellite Number	Imaging Mode	Polarization	Number of Scenes	Acquisition Date	Incidence Angle	Processor Version
Rosamond	Various	SM	HH	11	06/25/2021 - 03/15/2024	26.76 - 46.22	2.19.2 - 2.6.0
	C03, C05, C07, C08	SM	VV	22	03/27/2022 - 04/05/2023	28.41 - 47.87	2.21.1 - 2.38.5
	C03, C05, C07, C08	SP	HH	5	06/03/2021 - 06/09/2023	29.11 - 38.31	2.33.3 - 2.8.1
	C09, C10, C14	SS	HH	19	05/23/2024 - 06/04/2024	16.91 - 55.49	2.57.4
	C14	SS	VV	2	05/30/2024 - 06/05/2024	17.15 - 17.17	2.57.4
Oklahoma	C09, C10, C14	SM	HH	10	05/15/2024 - 05/28/2024	19.97 - 58.16	2.57.4
	C09, C10, C14	SS	HH	10	05/29/2024 - 06/07/2024	19.66 - 52.67	2.57.4
OPERA Site	C09, C10, C14	SM	HH	6	05/27/2024 - 06/08/2024	24.89 - 51.98	2.57.4
	C09, C10, C14	SM	VV	6	05/30/2024 - 06/04/2024	23.34 - 53.82	2.57.4
	C09, C10	SS	HH	6	05/23/2024 - 06/02/2024	28.20 - 54.51	2.57.4

The Rosamond array is located near the south end of the Rosamond dry lakebed in the desert of southern California (Fig. 5). The array consists of 38 triangular trihedral CRs in 3 sizes and oriented east or west, as depicted in Figure 5. Five 4.8-meter and five 0.7-meter CRs are oriented mostly eastward with an azimuth heading of 350°. The remaining five 0.7-m CRs have a heading angle of 90°. Of the twenty-three 2.4-meter CRs, ten face mostly east, while the remaining thirteen

are oriented west with an azimuth heading of 170°. Table 4 lists all the CRs used for the analysis at the Rosamond site.

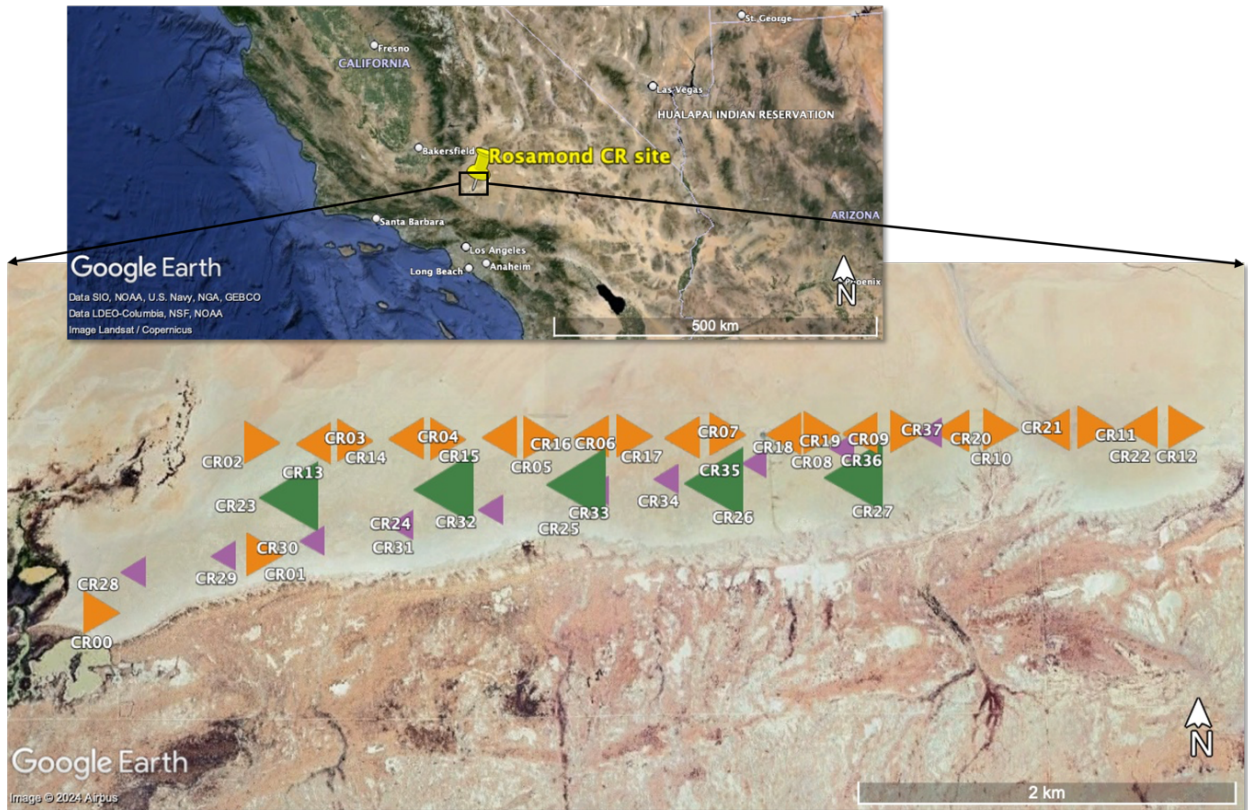


Figure 5. The upper image is a Google Earth overview of the location of the Rosamond CR array site in the Southern California desert. The lower image shows a closer view of the CR site, showing the CR names, alignment, and orientation.

Table 4. Corner Reflectors used for the analysis at the Rosamond site (Data collected 2023-12-13).

CR ID	Latitude (°)	Longitude (°)	Height Above Ellipsoid (m)	Orientation (°)	Elevation angle (°)	Size (m)
0	34.79696928	-118.0965308	660.7856	170.5	12.1	2.4384
1	34.79984853	-118.0869888	661.0345	170.5	8.72	2.4384
2	34.80523754	-118.0873892	660.7958	170	9.3	2.4384
3	34.80533834	-118.0819448	660.9918	170	8.63	2.4384
4	34.80541548	-118.0763782	661.1546	176	11.93	2.4384
5	34.8054937	-118.0708033	661.2243	171	11.07	2.4384
6	34.80558476	-118.0652258	661.2514	170	10.53	2.4384
7	34.80566746	-118.0596983	661.4008	170	14.7	2.4384
8	34.80575785	-118.0540222	661.5722	170.25	14.53	2.3989
9	34.80581413	-118.0489155	661.4449	175	10.63	2.4384
10	34.80592451	-118.043414	661.5768	170	14.6	2.4384
11	34.80602484	-118.0377366	661.7009	170	14.6	2.3989

12	34.80607395	-118.0323022	661.9127	169.5	8.1	2.4384
13	34.80519273	-118.0844198	660.9361	347	11.9	2.4384
14	34.80544015	-118.0789224	661.1566	350	16	2.4384
15	34.80552371	-118.0732806	661.3502	350.5	14.2	2.3989
16	34.80554864	-118.0678693	661.2834	350	8.03	2.4384
17	34.80555364	-118.0626289	661.3211	346	11	2.4384
18	34.80568769	-118.0564284	661.4424	346	8.97	2.4384
19	34.80572728	-118.0517598	661.5665	351.25	13.8	2.3989
20	34.80583804	-118.0463581	661.4455	350	10.77	2.4384
21	34.80590043	-118.0403334	661.4684	352	8.67	2.4384
22	34.80605059	-118.0351916	661.8013	9.8	16	2.4384
23	34.80250457	-118.0858055	661.1996	351.06	21	4.8
24	34.80290959	-118.0766468	661.4277	350.97	20.9	4.8
25	34.8031567	-118.0687806	661.5126	349.69	21	4.8
26	34.80322846	-118.0605826	661.6268	350.66	20.82	4.8
27	34.80351967	-118.0522806	661.646	349.64	20.93	4.8
28	34.79888379	-118.0948328	661.7686	9.9	15.05	0.8
29	34.79972489	-118.0895138	661.6029	91.5	34	0.7
30	34.80045797	-118.0843113	661.7026	91	33.8	0.7
31	34.80122329	-118.0790953	661.9545	351	16.7	0.7
32	34.80198195	-118.0737944	661.8988	90.5	33.2	0.7
33	34.80291898	-118.0675155	661.9962	354	20	0.7
34	34.80349615	-118.0633929	662.0635	354	21.9	0.7
35	34.80426739	-118.0581255	662.1272	91	31.6	0.7
36	34.80501201	-118.0528936	662.0533	92	31.5	0.7
37	34.80577951	-118.0476745	662.2021	351	28.1	0.7

The Oklahoma NISAR Calibration Array is distributed in North (Enid), Western (Clinton), and Southern (Lawton) Oklahoma (Fig. 6). Since June 2021, a total of seventeen (17) 2.8-m triangular trihedral CRs have been deployed. The sites listed in Table 5 are the CRs used in this analysis from the Oklahoma NISAR sites. Ten Stripmap scenes and ten Sliding Spotlight scenes were acquired over the Oklahoma sites. Each scene covers a different CR.

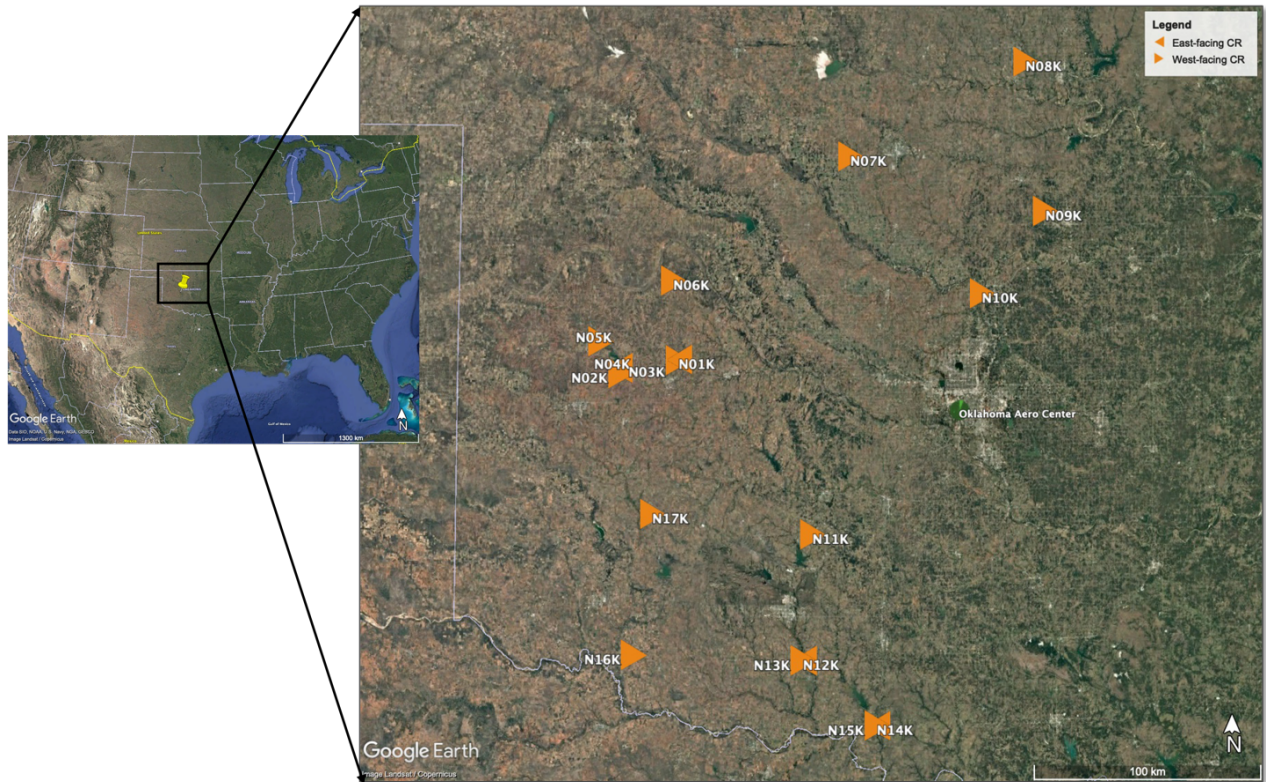


Figure 6. A Google Earth view of the NISAR Calibration array in Oklahoma. The triangles show CR names and distribution at the site.

Table 5. Corner Reflectors used for the analysis at the Oklahoma site (Data collected 2024-05-01).

O	Latitude (°)	Longitude (°)	Height Above Ellipsoid (m)	Orientation (°)	Elevation angle (°)	Size (m)
N02K	35.53645899	-99.21004135	481.1742	179.76	17.17	2.8
N04K	35.55705113	-99.21896408	475.6039	2.98	15.03	2.8

Corner reflectors were also installed at the Network of the Americas (NOTAs) international geophysics sensor network site of GPS and GNSS stations located along the San Andreas fault. These CRs are part of the NASA OPERA project for the purpose of calibrating InSAR timeseries measurements. Figure 7 and Table 6 show the CR locations installed at the OPERA calibration stations.

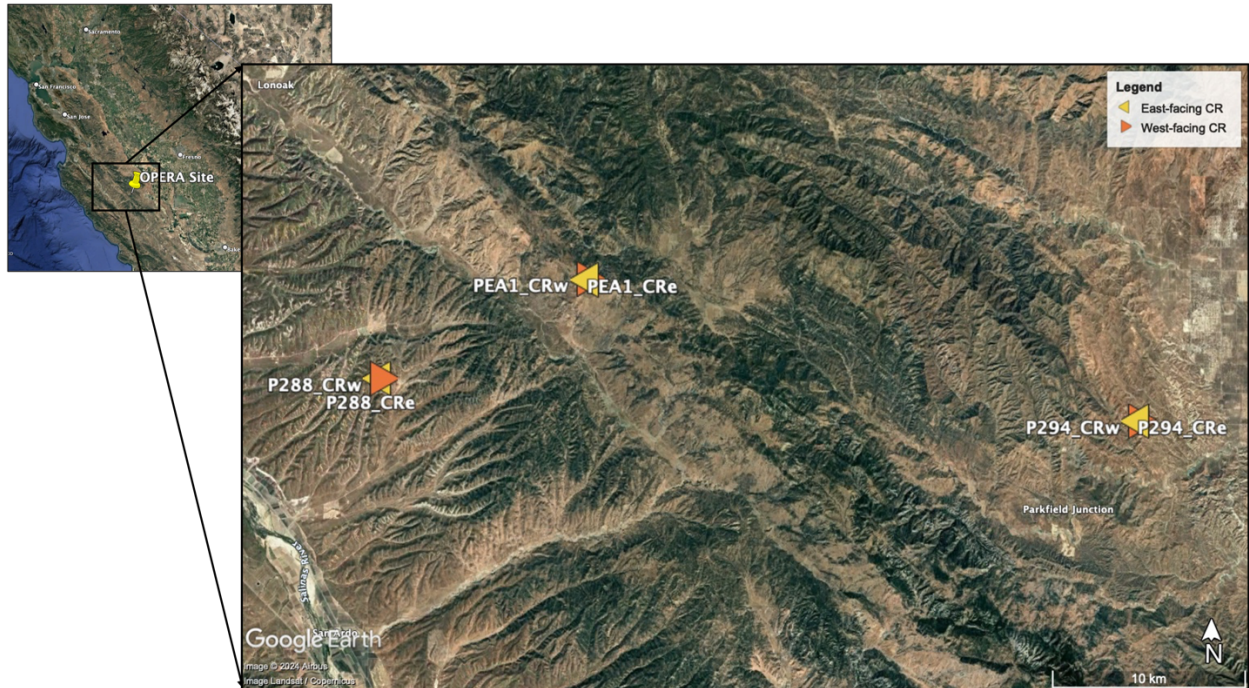


Figure 7. Google Earth view of the OPERA calibration stations located in the central coastal California mountains.

Table 6. Corner Reflectors used for the analysis at the OPERA calibration site.

CR ID	Latitude (°)	Longitude (°)	Height Above Ellipsoid (m)	Orienta- tion (°)	Elevation angle (°)	Size (m)
PEA1_CRw	36.18750838	-120.7589888	779.715	178	13.4	2.4
PEA1_CRe	36.18709	-120.758342	788.469	360	16.5	2.4
P288_CRw	36.14044255	-120.8792075	398.389	183	15.5	2.4
P288_CRe	36.14042406	-120.8791667	398.412	355	14.8	2.4
P294_CRw	36.12332979	-120.4398813	507.177	182	15.4	2.4
P294_CRe	36.12333793	-120.4398392	506.966	359	15.1	2.4

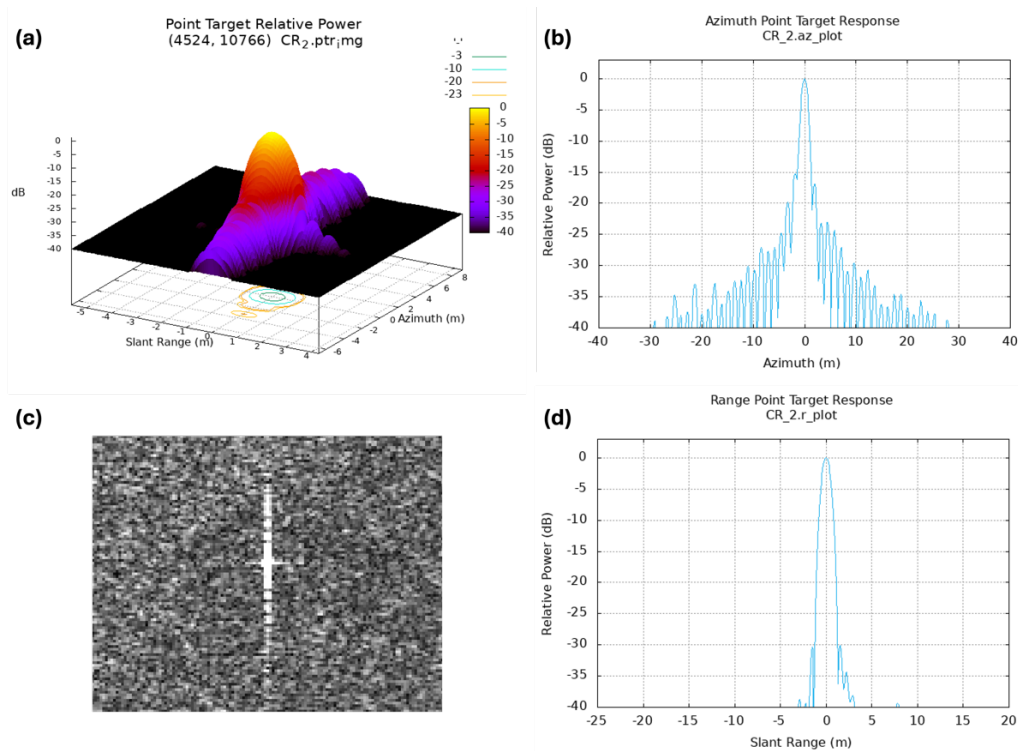
4.1 Spatial Resolution

4.1.1 Method

The spatial resolution of the imagery was validated using point target analysis tools provided in GAMMA software, such as the SLC version of the point target analysis command, *ptarg_SLC*, which estimates the 3 dB peak widths in range and azimuth for a given corner reflector. Assessment of the spatial resolution was performed for three dedicated calibration sites with installed CRs, a) Rosamond, CA b) Oklahoma, and c) OPERA calibration site.

Figure 8 provides an example of the IRF analysis over CR02 (2.4-m) at the Rosamond site. We found that sidelobes in the range direction were very low after the Avci-Nacaroglu exponential function was applied (Avci and Nacaroglu, 2008). The Capella metadata includes parameters for

the filters used, although the observed measurements appear to feature much better sidelobe performance than what appears in the parameterization of the Avci-Nacaroglu filter in the metadata. To accurately analyze the IRF of corner reflector signals, the SLC image was oversampled by a factor of 8 in both range and azimuth directions. Oversampling increases the number of pixels in the image, effectively interpolating the data to allow for more precise measurement of the point target response. The *ptarg_SLC* estimates the 3 dB peak widths in range and azimuth, which is the spatial resolution of the SLC image, as well as the PSLR and ISLR.



Scene ID: CAPELLA_C05_SM_SLC_VV_20220402223614_20220402223618

Figure 8. Example of point target analysis using GAMMA *ptarg_SLC* module. This example shows IRF of CR02 at the Rosamond site from scene ID CAPELLA_C05_SM_SLC_VV_20220402223614_20220402223618. (a) 3D plot of CR02 relative power; (b) azimuth point target response plot; (c) CR02 in the SLC image; (d) the range point target response plot.

4.1.2 Results Compliance

Table 7 shows the quality values related to the spatial resolution provided in the Capella Space SAR Imagery Products Guide (Capella Space, 2022). The range resolution is given in slant range direction for SLC data.

Table 7. Specification of the standard single look complex (SLC) image product type

Imaging Mode	Nominal Scene Size	Azimuth Resolution [m]	Slant Range Resolution [m]	Look Angle Range
Spotlight	5 km x 5 km	0.5	0.3	25° to 40°
Sliding Spotlight	5 km x 10 km	1.0	0.5	25° to 40°
Stripmap	5 km x 20 km	1.2	0.75	25° to 40°

The IRF quality parameters, PSLR and ISLR, for Capella satellites are not provided in the Capella product guide documentation. Instead, the reference values for PSLR and ISLR were simulated using the vendor-provided window parameters in the extended metadata (Table 8). The Capella images we acquired were generated by applying either the Avci-Nacaroglu or rectangular windowing function in the range direction and either the antenna-taper or rectangular windowing function in the azimuth direction. The nominal parameters for the Avci-Nacaroglu window use an α value of 1.25. Based on the metadata, the following PSLR and ISLR values are generated for typical configurations with the associated parameters. Figure 9 shows the impulse response generated by two windowing functions below.

Table 8. Simulated PSLR and ISLR values based on windowing parameters.

Window	PSLR (dB)	ISLR (dB)	Parameters
Avci-Nacaroglu	-18.38	-16.49	$\alpha = 1.25$
Rectangular	-13.31	-9.69	N/A

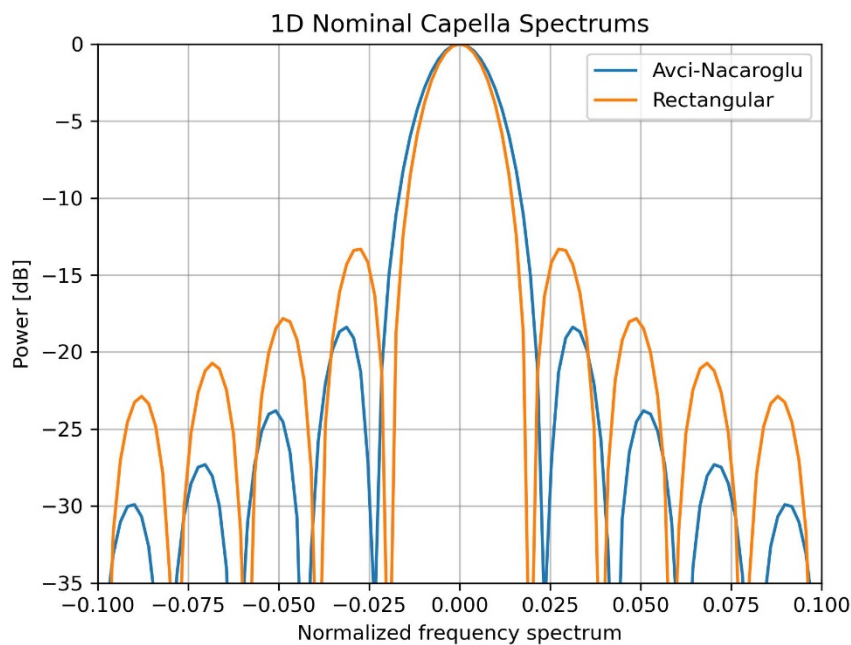


Figure 9. Simulated impulse response using Avci-Nacaroglu and Rectangular windowing functions provided by typical Capella metadata parameters.

From this analysis it can be seen that the reconstruction of Capella’s IRF is achievable through use of the associated metadata by a subject matter expert. The Capella Space metadata generally follows standard naming conventions. However, some sections of the metadata appear to have inconsistent naming conventions, such as swapped values for column and row pixel spacing for some of the images processed using the PFA algorithm, or the use of SS for Sliding Spotlight products in the product name but listing SL in the Capella SAR Product Format Specification (Capella Space, 2023).

Tables 9, 10, and 11 show the observed spatial resolution, PSLR, and ISLR of each Capella Space image used for the evaluation sites.

4.1.2.1 Rosamond, CA, USA

Table 9 provides the results we obtained over RCRA and includes SM, SP, and SS data. Overall, the measured range and azimuth resolutions are close to the expected values. The PSLR and ISLR values vary depending on the windowing functions used as discussed in section 4.1.2.

Table 9. Observed spatial resolution, PSLR and ISLR values in azimuth and range directions over Rosamond, CA.

Sat. #	Im. Mode	Pol	Acquisition Date	Rg Res. [m]	Az Res. [m]	Rg PSLR [dB]	Az PSLR [dB]	Rg ISLR [dB]	Az ISLR [dB]
C02	SM	HH	20210727	1.35±0.10	1.18±0.10	-12.81±0.66	-15.44±3.33	-11.32±0.67	-14.46±2.97
C03	SM	HH	20210625	0.98±0.07	1.17±0.09	-26.05±6.90	-17.36±2.08	-26.68±7.88	-16.38±2.19
C03	SM	VV	20220530	0.99±0.07	1.27±0.07	-26.04±7.21	-14.67±2.19	-26.16±8.50	-13.28±2.14
C03	SM	VV	20220626	0.98±0.05	1.23±0.07	-30.11±3.74	-16.49±0.33	-31.37±4.08	-14.91±1.01
C03	SM	HH	20220818	0.96±0.05	1.23±0.04	-31.49±1.51	-15.76±0.44	-31.83±2.08	-14.31±0.18
C05	SM	VV	20220402	0.96±0.03	1.24±0.07	-29.40±2.64	-14.86±0.88	-29.04±3.54	-13.69±1.15
C05	SM	HH	20220709	0.98±0.04	1.27±0.06	-29.40±4.62	-16.88±3.23	-29.62±5.28	-14.87±1.46
C05	SM	VV	20220811	0.95±0.07	1.24±0.06	-29.05±4.05	-16.00±0.79	-29.75±3.97	-14.38±1.11
C05	SM	HH	20221214	0.70±0.05	1.21±0.08	-13.11±0.32	-15.85±1.58	-11.33±0.49	-14.06±0.80
C07	SM	HH	20220327	0.95±0.06	1.32±0.08	-27.19±4.17	-15.67±2.28	-29.02±4.70	-14.23±1.40
C07	SM	VV	20220507	0.96±0.05	1.27±0.07	-27.29±3.22	-16.23±1.02	-28.81±4.50	-14.79±0.82
C07	SM	VV	20220610	0.97±0.05	1.26±0.08	-28.43±1.57	-16.69±0.26	-30.20±1.18	-15.29±0.24
C07	SM	VV	20220617	0.95±0.05	1.27±0.07	-27.83±0.61	-16.34±1.72	-29.58±1.31	-14.97±1.87
C07	SM	VV	20220803	0.98±0.06	1.25±0.07	-27.72±4.53	-16.09±1.62	-29.58±4.87	-14.95±0.76
C07	SM	VV	20220907	0.94±0.04	1.24±0.08	-24.70±1.96	-16.40±0.60	-25.98±2.98	-15.19±0.32
C07	SM	VV	20221013	0.96±0.04	1.21±0.06	-24.28±0.96	-17.77±0.46	-20.95±0.71	-16.33±0.33
C07	SM	VV	20221022	0.93±0.04	1.18±0.07	-22.88±0.88	-17.43±0.36	-18.35±0.80	-16.30±0.25
C07	SM	VV	20221221	0.67±0.04	1.18±0.08	-12.34±0.41	-17.58±0.47	-10.78±0.37	-16.42±0.45
C07	SM	VV	20230310	1.61±0.07	1.15±0.07	-13.07±0.55	-17.51±0.44	-10.37±0.44	-16.32±0.73
C07	SM	VV	20230405	1.46±0.04	1.17±0.08	-13.30±0.71	-17.20±1.19	-12.20±0.78	-15.96±0.95
C08	SM	HH	20220319	0.97±0.05	1.31±0.08	-30.55±1.80	-15.58±1.82	-30.31±2.15	-14.07±1.14
C08	SM	VV	20220327	0.96±0.05	1.25±0.06	-31.11±0.76	-16.38±1.00	-31.16±1.14	-14.96±0.90
C08	SM	VV	20220410	0.97±0.05	1.26±0.11	-28.37±6.59	-14.40±2.27	-27.76±7.46	-13.25±2.00
C08	SM	VV	20220521	0.98±0.04	1.23±0.06	-30.76±1.08	-16.85±0.29	-30.66±1.46	-15.45±0.30
C08	SM	VV	20220724	0.95±0.04	1.28±0.09	-31.06±0.87	-16.59±0.64	-31.06±0.71	-14.07±0.57
C08	SM	VV	20221031	0.95±0.05	1.15±0.06	-27.78±5.80	-16.86±1.62	-27.28±6.87	-15.70±1.21
C08	SM	VV	20221108	0.96±0.05	1.17±0.07	-29.54±4.40	-17.04±1.96	-29.61±4.84	-15.84±1.52
C08	SM	HH	20221218	0.70±0.07	1.21±0.09	-12.95±1.74	-16.45±1.96	-11.30±1.44	-15.00±2.22
C08	SM	VV	20230120	0.66±0.05	1.22±0.07	-13.51±0.24	-18.40±0.40	-11.65±0.12	-17.26±0.29
C08	SM	VV	20230317	0.67±0.05	1.21±0.05	-13.52±0.07	-18.53±0.23	-11.67±0.05	-17.33±0.13
C09	SM	HH	20240205	0.69±0.07	1.33±0.39	-11.85±1.20	-14.01±2.58	-10.43±1.15	-13.39±2.59
C09	SM	HH	20240218	0.68±0.05	1.24±0.19	-12.43±0.99	-15.38±2.76	-10.65±0.96	-15.05±3.27
C10	SM	HH	20240315	0.73±0.04	1.23±0.22	-13.38±2.51	-14.86±3.29	-12.57±2.00	-14.00±2.81

Sat. #	Im. Mode	Pol	Acquisition Date	Rg Res. [m]	Az Res. [m]	Rg PSLR [dB]	Az PSLR [dB]	Rg ISLR [dB]	Az ISLR [dB]
C03	SP	HH	20210603	0.41±0.02	0.47±0.05	-20.69±6.14	-12.70±1.16	-20.59±6.66	-11.08±1.01
C03	SP	HH	20210917	0.49±0.03	0.45±0.04	-23.89±4.78	-12.70±1.18	-23.20±5.85	-11.09±0.83
C05	SP	HH	20221206	0.28±0.02	0.46±0.03	-12.23±1.71	-10.99±0.42	-12.22±0.95	-8.90±0.24
C07	SP	HH	20230609	0.31±0.03	0.44±0.03	-13.96±0.99	-12.84±0.62	-13.77±1.07	-11.43±0.62
C08	SP	HH	20221231	0.29±0.04	0.49±0.09	-11.39±1.07	-12.40±1.64	-11.54±0.87	-11.22±1.05
C09	SS	HH	20240523	0.46±0.06	0.44±0.05	-10.93±1.36	-15.69±3.01	-9.29±0.75	-15.93±3.22
C09	SS	HH	20240526	0.44±0.03	0.41±0.05	-11.33±0.89	-14.65±3.17	-9.73±0.65	-13.76±3.19
C09	SS	HH	20240527	0.44±0.02	0.80±0.11	-11.23±0.63	-15.05±2.60	-9.37±0.53	-14.45±3.66
C09	SS	HH	20240528	0.45±0.05	0.84±0.13	-11.29±0.82	-15.08±2.71	-9.57±0.49	-14.61±3.54
C09	SS	HH	20240601	0.45±0.03	0.47±0.06	-11.53±1.15	-15.09±2.47	-9.46±0.77	-14.60±2.50
C10	SS	HH	20240525	0.52±0.06	0.79±0.09	-15.91±2.13	-13.82±1.81	-14.12±2.26	-12.45±2.29
C10	SS	HH	20240527	0.50±0.03	0.40±0.05	-16.51±0.77	-13.89±2.78	-15.07±0.94	-14.15±3.42
C10	SS	HH	20240530	0.49±0.03	0.76±0.06	-16.00±1.16	-13.97±1.16	-14.53±1.07	-12.83±2.23
C10	SS	HH	20240530	0.50±0.04	0.84±0.09	-14.45±3.12	-14.63±2.16	-13.26±2.71	-14.37±2.42
C10	SS	HH	20240604	0.48±0.03	0.75±0.08	-15.57±2.02	-13.34±2.08	-13.79±1.71	-12.35±1.92
C14	SS	HH	20240524	0.47±0.02	0.76±0.08	-13.08±1.41	-13.78±1.77	-11.52±1.18	-12.57±2.59
C14	SS	HH	20240525	0.46±0.03	0.43±0.06	-13.83±1.38	-14.71±2.11	-12.24±1.09	-15.18±2.77
C14	SS	HH	20240526	0.47±0.03	0.44±0.06	-13.43±1.25	-13.11±2.97	-12.32±1.09	-12.91±2.88
C14	SS	HH	20240527	0.45±0.02	0.80±0.14	-13.43±1.56	-13.94±2.44	-12.08±1.05	-13.32±2.95
C14	SS	HH	20240529	0.47±0.04	0.42±0.06	-12.99±1.66	-14.99±3.64	-11.53±1.48	-13.97±3.02
C14	SS	VV	20240530	0.45±0.05	0.81±0.10	-13.62±1.40	-14.47±2.26	-11.91±1.15	-13.65±3.23
C14	SS	HH	20240531	0.46±0.03	0.41±0.07	-14.01±1.25	-14.44±3.27	-12.56±0.75	-14.34±3.58
C14	SS	HH	20240601	0.48±0.05	0.43±0.04	-13.54±1.38	-12.10±2.20	-12.05±1.07	-11.92±2.31
C14	SS	HH	20240604	0.46±0.05	0.43±0.07	-12.89±1.71	-12.81±2.46	-11.61±1.38	-12.49±2.44
C14	SS	VV	20240605	0.46±0.03	0.76±0.09	-13.45±1.39	-13.40±1.69	-11.87±1.04	-12.54±2.52

Figure 10 shows an example of one of the point target images showing abnormal focusing. While the spatial resolution of almost all the images meets the specifications provided in the documentation by Capella, the range compression of a couple of images appears abnormal, and the slant range resolution was lower than expectation. The scenes showing a similar issue are C07_SM_20230310 and C07_SM_20230405. The slant range resolutions measured from the CRs in these scenes are approximately 1.4 to 1.6 m.

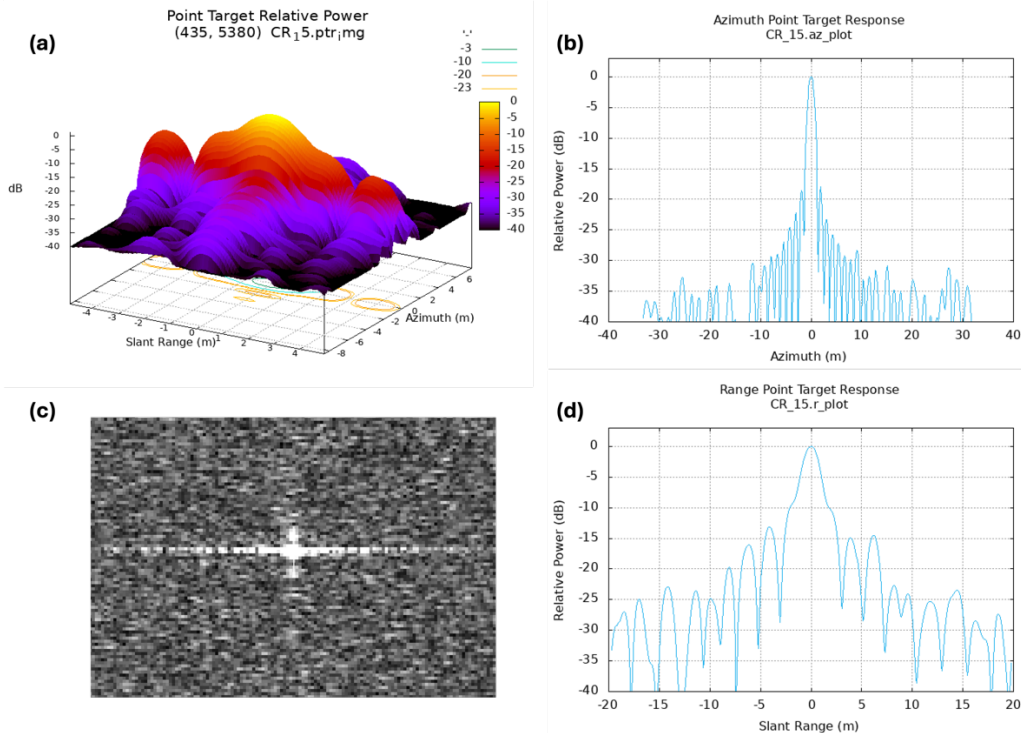


Figure 10. Point target showing abnormal focusing in the range direction from scene ID CAPELLA_C07_SM_SLC_VV_20230310051642_20230310051646. This example shows the point target CR15 at the Rosamond site. (a) 3D plot of CR15 relative power ; (b) azimuth point target response plot; (c) CR15 in the SLC image; (d) the range point target response plot.

We also identified a double peak from the 4.8 m CRs in a few of the SM images. Figure 11 shows an example of the point target with a double peak. The IRF quality parameters from those images with a double peak were very poor and did not meet the expected values in the azimuth direction. Therefore, those CRs were excluded from the statistics. The scenes that showed the double peak issue were C02_SM_20210727, C09_SM_20240205, C09_SM_20240218, and C10_SM_20240315. Although further investigation is needed, the evaluation team noticed that these scenes with underperforming IRF were acquired with a heading angle between 113° and 118°, while all well-performing scenes were acquired with a heading of approximately -12°. Considering the orientation of the CRs at the Rosamond site, we assume that this issue could be induced by geometric misalignment between the CR pointing and SAR line-of-sight.

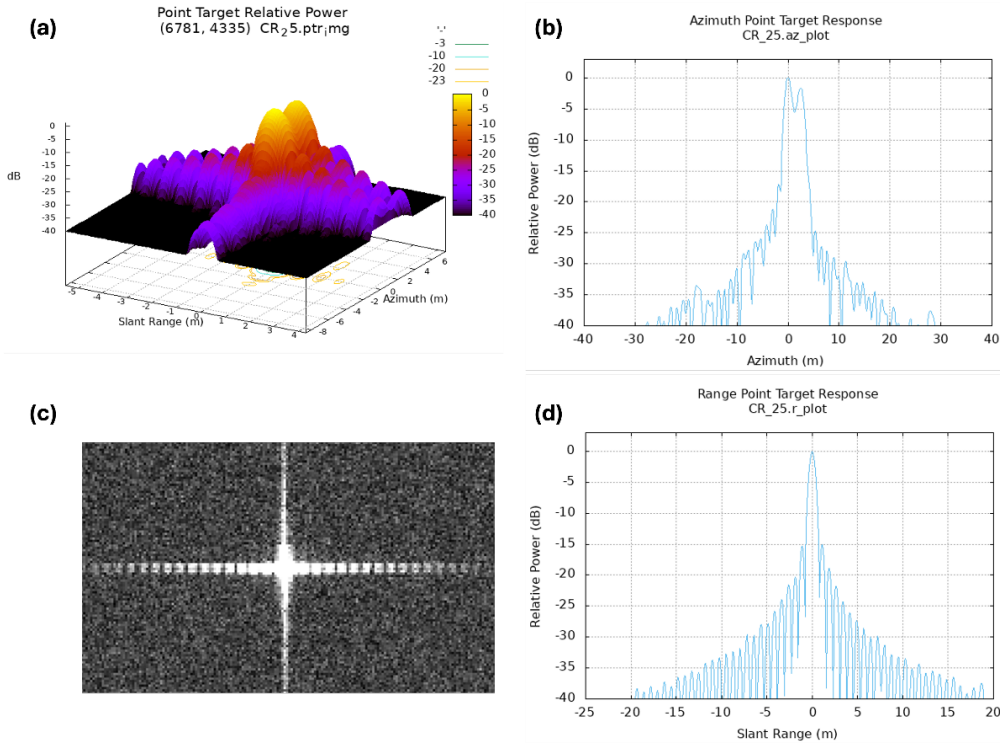


Figure 11. Point target showing a double peak in azimuth direction from scene ID CAPELLA_C10_SM_SLC_HH_20240315165611_20240315165614. This example shows point target CR25 at the Rosamond site. (a) 3D plot of CR25 relative power; (b) azimuth point target response plot; (c) CR25 in the SLC image; (d) the range point target response plot.

The scene ID CAPELLA_C05_SM_SLC_HH_20210804092225_20210804092229 was also analyzed, but due to potential focusing issues, the measured IRF parameters from the CRs were not reasonable. Thus, this scene was also excluded from the statistics table.

4.1.2.2 Oklahoma, USA

Table 10 shows the IRF analysis results for the Oklahoma site. Several Capella images over the Oklahoma site were excluded from this IRF analysis, as the CRs were either not observed or had very weak signals in the scenes due to the geometry. Therefore, only images showing point target signals from the CRs were used for the analysis. The scenes that were excluded from Table 10 were C09_SM_20240518, C10_SM_20240525, C14_SM_20240515, C14_SM_20240518, C14_SM_20240525, C14_SM_20240528, C09_SS_20240603, C10_SS_20240601, and C14_SS_20240602.

Table 10. Observed spatial resolution, PSLR and ISLR values in azimuth and range directions over Oklahoma.

Sat. #	Im. Mode	Pol	Acquisition Date	Rg Res. [m]	Az Res. [m]	Rg PSLR [dB]	Az PSLR [dB]	Rg ISLR [dB]	Az ISLR [dB]
C09	SM	HH	20240526	0.683	1.15	-12.808	-17.001	-10.751	-15.916
C09	SM	HH	20240528	0.812	1.089	-10.177	-10.704	-8.81	-10.276
C14	SM	HH	20240523	0.665	1.305	-13.734	-16.84	-11.934	-15.687
C14	SM	HH	20240527	0.67	1.257	-10.838	-12.79	-9.55	-11.114

Sat. #	Im. Mode	Pol	Acquisition Date	Rg Res. [m]	Az Res. [m]	Rg PSLR [dB]	Az PSLR [dB]	Rg ISLR [dB]	Az ISLR [dB]
C09	SS	HH	20240601	0.612	0.804	-9.006	-14.591	-8.701	-12.517
C09	SS	HH	20240607	0.443	0.74	-11.569	-16.314	-9.151	-15.211
C10	SS	HH	20240531	0.524	0.689	-11.68	-11.103	-10.77	-8.541
C10	SS	HH	20240604	0.542	1.157	-16.385	-22.66	-15.259	-22.602
C14	SS	HH	20240529	0.455	0.689	-14.605	-14.337	-12.88	-13.962
C14	SS	HH	20240601	0.493	0.751	-14.245	-13.787	-12.542	-12.1
C14	SS	HH	20240604	0.426	0.745	-14.288	-13.69	-12.554	-11.933

4.1.2.3 OPERA Calibration site, CA, USA

Table 11 provides the results we obtained over OPERA CRs and includes SM, and SS data. Overall, the measured range and azimuth resolutions are close to the expected values. The PSLR and ISLR values vary depending on the windowing functions used.

Table 11. The IRF analysis for the OPERA Calibration site; average and standard deviation of all observed CRs.

Sat. #	Im. Mode	Pol	Acquisition Date	Rg Res. [m]	Az Res. [m]	Rg PSLR [dB]	Az PSLR [dB]	Rg ISLR [dB]	Az ISLR [dB]
C09	SM	VV	20240602	0.689	1.526	-10.179	-11.339	-8.069	-9.292
C09	SM	VV	20240603	0.694	1.159	-12.635	-16.295	-10.838	-16.108
C09	SM	VV	20240604	0.623	1.166	-12.484	-16.853	-10.65	-15.615
C09	SM	HH	20240607	0.66	1.212	-13.261	-18.674	-11.578	-17.982
C10	SM	VV	20240531	0.683	1.217	-15.507	-9.893	-13.674	-9.737
C10	SM	HH	20240606	0.645	1.077	-15.211	-17.1	-13.616	-16.227
C14	SM	HH	20240527	0.705	1.565	-13.855	-17.107	-12.034	-15.918
C14	SM	VV	20240530	0.707	1.134	-13.856	-16.524	-12.057	-15.703
C14	SM	VV	20240602	0.624	1.655	-13.815	-15.395	-12.038	-16.638
C14	SM	HH	20240605	0.654	1.443	-13.772	-16.658	-12.011	-16.661
C14	SM	HH	20240608	0.746	1.248	-13.797	-16.806	-12.207	-15.712
C09	SS	HH	20240529	0.415	0.456	-11.021	-17.614	-8.84	-17.935
C09	SS	HH	20240602	0.461	0.835	-9.72	-15.955	-8.984	-15.191
C10	SS	HH	20240526	0.503	1.054	-16.483	-10.942	-15.096	-12.293
C10	SS	HH	20240601	0.52	0.87	-16.599	-15.261	-15.168	-15.19
C10	SS	HH	20240601	0.489	0.498	-16.488	-9.085	-15.023	-9.468

In addition to the scenes listed in Table 11, we also analyzed the C10_SM_20240605 and C09_SS_20240523 scenes, which showed the double peak issue in azimuth. Therefore, those two images were excluded from the list.

Summary of Spatial Resolution Assessment

The overall spatial resolution performance of Capella satellite imagery is assessed to be excellent. The spatial resolution in range and azimuth directions for almost all images was close or in line with the values provided in the Capella documentation. However, approximately 75% of SM mode images from the Rosamond site measured slightly lower slant range resolutions than the expected value of 0.75 meters for SM mode imagery.

Sidelobe levels measured from the CRs are greater or consistent with the theoretical performance of Capella imagery. The PSLR and ISLR values close to -30 dB were measured from images where the Avci-Nacaroglu window was applied, which is lower than the value of -18 dB that was calculated from the simulation results in section 4.1.2. Two images in SP mode, C03_SP_20210603 and C03_SP_20210917, measured approximately -20 dB, and fall within the expected theoretical performance range. Additionally, the images with the rectangular window measured sidelobe levels close to -13 dB, which is also close to the expected theoretical performance.

4.2 Geolocation Accuracy

4.2.1 Method

The geolocation accuracy was calculated based on the known and image-based measurement location of the corner reflectors at the test sites. The assessment of the Capella imagery was performed using the GAMMA Remote Sensing software and its SLC point target analysis tool, *ptarg_SLC*. Python code developed internally at GSFC was used to analyze images with geocoding errors larger than 16 pixels to provide an initial estimation of the CR location. The expected location of the corner reflectors (red plus sign) on the SAR image was calculated based on the geographical coordinates of the reflector, and the image metadata and were compared to the measured CR image coordinate (green plus sign) on the SAR image (Figure 12). The geolocation errors were measured in range and azimuth direction separately in absolute values, and the absolute location error (ALE) was then calculated by the equation below:

$$ALE = \sqrt{(Err_{rg, mean})^2 + (Err_{az, mean})^2}$$

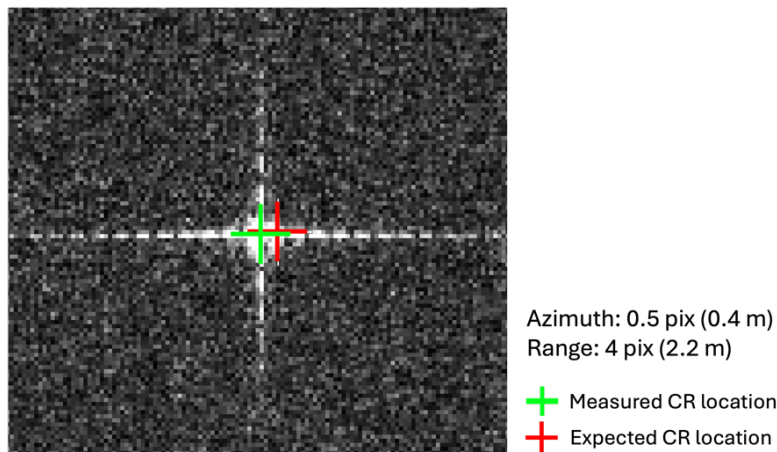


Figure 12. Geolocation accuracy assessment with GAMMA software. The example point target is in the scene ID CAPELLA_C09_SM_SLC_HH_20240218035539_20240218035541. The expected CR location (red plus sign) is compared with the observed location in the Capella SAR image (green plus sign).

4.2.2 Results Compliance

The performance specification related to the geolocation accuracy is not provided in the Capella documentation. In the technical note for Capella assessment by ESA EDAP, the geolocation errors in range and azimuth were assessed to be within 4 m (ESA, 2022).

Tables 12, 13, and 14 show the measured geolocation errors from the test sites. Table 12, which presents the analysis results for the Rosamond site, shows the average and standard deviation values from all CRs observed in the scenes. Additionally, Tables 13 and 14, for the Oklahoma and the OPERA sites, respectively, present the geolocation errors from individual CRs observed in each image. Scenes showing larger errors than the reported values from Capella are highlighted in red text.

4.2.1.1 Rosamond, CA, USA

For the Rosamond site, we analyzed 33 SM, 5 SP, and 21 SS images to calculate geolocation errors. On average, the ALE is 2.4 m, 2.1 m, and 1.2 m respectively for SM, SP and SS imagery. Table 12 lists the results of the geolocation accuracy analysis for the various Capella satellites over the Rosamond site. The table includes the average and the standard deviation of all observed CRs of the scenes. Scenes with larger than expected errors are highlighted in red.

Table 12. Rosamond geolocation accuracy analysis for Capella Space; average and standard deviation of all observed CRs.

Satellite Number	Image Mode	Pol	Acquisition Date	Range Location Error [m]	Azimuth Location Error [m]	Absolute Location Error [m]
C02	SM	HH	20210727	0.87±0.07	0.42±0.16	0.97
C03	SM	HH	20210625	0.11±0.13	1.48±0.08	1.48
C03	SM	VV	20220530	1.59±0.05	1.89±0.12	2.47
C03	SM	VV	20220626	2.71±0.03	1.43±0.09	3.06
C03	SM	HH	20220818	2.48±0.03	0.43±0.04	2.52
C05	SM	VV	20220402	0.63±0.02	0.77±0.07	0.99
C05	SM	HH	20220709	2.34±0.15	0.76±0.09	2.46
C05	SM	VV	20220811	2.72±0.03	0.45±0.03	2.76
C05	SM	HH	20221214	1.43±0.35	0.30±0.21	1.46
C07	SM	HH	20220327	2.66±0.03	4.39±0.06	5.13
C07	SM	VV	20220507	2.74±0.11	1.86±0.04	3.31
C07	SM	VV	20220610	3.11±0.03	2.27±0.05	3.85
C07	SM	VV	20220617	2.23±0.03	2.92±0.06	3.67
C07	SM	VV	20220803	3.74±0.08	2.63±0.06	4.57
C07	SM	VV	20220907	2.79±0.03	1.11±0.04	3.00
C07	SM	VV	20221013	1.19±0.03	0.41±0.04	1.26
C07	SM	VV	20221022	1.05±0.02	0.16±0.05	1.06
C07	SM	VV	20221221	0.20±0.02	0.23±0.05	0.30
C07	SM	VV	20230310	10.37±0.05	11.27±0.04	15.32
C07	SM	VV	20230405	0.94±0.03	0.34±0.05	1.00
C08	SM	HH	20220319	1.68±0.03	0.22±0.07	1.69
C08	SM	VV	20220327	2.53±0.02	0.25±0.04	2.54
C08	SM	VV	20220410	0.71±0.04	1.47±0.05	1.63

C08	SM	VV	20220521	3.60±0.03	1.86±0.05	4.05
C08	SM	VV	20220724	2.34±0.03	1.40±0.04	2.73
C08	SM	VV	20221031	2.46±0.03	1.24±0.04	2.75
C08	SM	VV	20221108	1.60±0.03	0.07±0.05	1.60
C08	SM	HH	20221218	2.43±0.17	0.18±0.09	2.44
C08	SM	VV	20230120	1.83±0.02	0.11±0.06	1.83
C08	SM	VV	20230317	1.55±0.01	0.52±0.03	1.63
C09	SM	HH	20240205	3.28±0.07	5.10±0.55	6.06
C09	SM	HH	20240218	2.17±0.08	0.70±0.50	2.28
C10	SM	HH	20240315	0.61±0.14	0.22±0.50	0.65
C03	SP	HH	20210603	1.70±0.46	1.12±0.32	2.04
C03	SP	HH	20210917	0.68±0.21	1.08±0.23	1.28
C05	SP	HH	20221206	1.47±0.09	0.41±0.08	1.53
C07	SP	HH	20230609	2.24±0.03	1.67±0.05	2.79
C08	SP	HH	20221231	2.44±0.13	0.21±0.07	2.45
C09	SS	HH	20240523	0.42±0.04	0.41±0.06	0.59
C09	SS	HH	20240526	0.41±0.14	1.00±1.05	1.08
C09	SS	HH	20240527	0.34±0.06	0.21±0.17	0.40
C09	SS	HH	20240528	0.14±0.04	1.08±0.38	1.09
C09	SS	HH	20240601	0.53±0.16	0.96±1.12	1.10
C10	SS	HH	20240525	0.66±0.09	0.89±0.85	1.11
C10	SS	HH	20240527	0.64±0.03	0.24±0.05	0.68
C10	SS	HH	20240530	0.43±0.05	0.22±0.15	0.48
C10	SS	HH	20240530	0.49±0.11	0.52±0.75	0.71
C10	SS	HH	20240604	0.90±0.06	0.65±0.60	1.11
C14	SS	HH	20240524	0.04±0.03	0.33±0.19	0.33
C14	SS	HH	20240525	1.00±0.04	0.60±0.08	1.17
C14	SS	HH	20240526	0.29±0.09	0.63±0.92	0.69
C14	SS	HH	20240527	2.26±0.04	6.02±0.20	6.43
C14	SS	HH	20240529	0.57±0.23	3.76±0.91	3.80
C14	SS	VV	20240530	0.09±0.11	0.17±0.16	0.19
C14	SS	HH	20240531	0.20±0.04	0.38±0.07	0.43
C14	SS	HH	20240601	0.13±0.07	1.10±1.13	1.11
C14	SS	HH	20240604	0.67±0.09	0.70±1.07	0.97
C14	SS	VV	20240605	0.05±0.09	0.58±0.18	0.58

Figure 13 shows plotted azimuth and slant range errors from SM, SP and SS mode imagery as shown in Table 12. The data point collected from a C07 image, shown in red in Table 12, is not shown in Figure 13 because it was beyond the bounds of both figure axes.

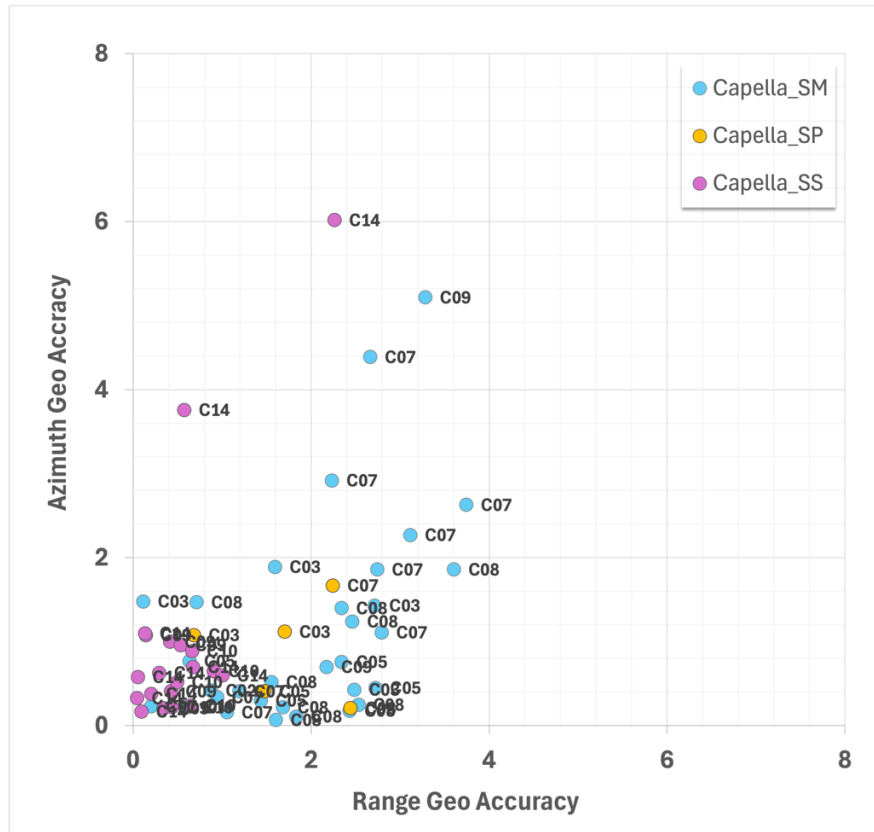


Figure 13. Geolocation errors of Capella SM, SP, and SS mode images. Each plot shows the mean value of all CRs observed in an image. Scenes showing very large geolocation errors or a focusing issue were excluded from the plots (C05_SM_20210804, C07_SM_20230310, C14_SS_20240523).

4.2.1.2 Oklahoma, USA

Table 13 shows the results obtained over the Oklahoma CRs using 10 SM and 10 SS images. On average the ALE is 1.0 m, and 1.2 m, respectively, for SM and SS imagery.

Table 13. Geolocation accuracy analysis over the Oklahoma site; the values are calculated from a single CR observed within a scene.

Satellite Number	Image Mode	Pol	Acquisition Date	Range Location Error [m]	Azimuth Location Error [m]	Absolute Location Error [m]
C09	SM	HH	20240526	0.1315	0.6765	0.69
C09	SM	HH	20240528	0.0650	0.6850	0.69
C14	SM	HH	20240523	1.9506	1.2963	2.34
C14	SM	HH	20240527	0.1785	0.0271	0.18
C09	SS	HH	20240601	0.2281	0.4051	0.46
C09	SS	HH	20240607	0.2163	0.8161	0.84
C10	SS	HH	20240531	0.0038	0.2810	0.28
C10	SS	HH	20240604	0.6905	0.2633	0.74
C14	SS	HH	20240529	1.0922	1.4937	1.85
C14	SS	HH	20240601	2.3071	2.8354	3.66
C14	SS	HH	20240604	0.0792	0.1692	0.19

4.2.1.3 OPERA calibration site, CA, USA

Table 14 shows the results obtained over the OPERA CRs using 12 SM and 6 SS images. On average the ALE is 1.5 m and 1.9 m, respectively, for SM and SS imagery.

Table 14. Geolocation accuracy analysis over the OPERA calibration site; the values are calculated from a single CR observed within a scene.

Satellite Number	Image Mode	Pol	Acquisition Date	Range Location Error [m]	Azimuth Location Error [m]	Absolute Location Error [m]
C09	SM	VV	20240602	0.9009	0.1818	0.92
C09	SM	VV	20240603	0.1188	1.4429	1.45
C09	SM	VV	20240604	0.0024	0.7800	0.78
C09	SM	HH	20240607	1.1536	0.5860	1.29
C10	SM	VV	20240531	0.4752	0.1178	0.49
C10	SM	HH	20240606	0.0779	2.7280	2.73
C14	SM	HH	20240527	0.3605	0.9889	1.05
C14	SM	VV	20240530	1.4751	1.4210	2.05
C14	SM	VV	20240602	0.4876	0.0176	0.49
C14	SM	HH	20240605	2.5902	4.2532	4.98
C14	SM	HH	20240608	0.4236	0.5041	0.66
C09	SS	HH	20240529	0.0330	3.8701	3.87
C09	SS	HH	20240602	0.1547	0.0259	0.16
C10	SS	HH	20240526	0.0445	1.6108	1.61
C10	SS	HH	20240601	0.1946	0.7839	0.81
C10	SS	HH	20240601	0.8941	2.7997	2.94

Summary of Geolocation Accuracy Assessment

As a result of evaluating the geolocation accuracy of Capella satellite imagery, the overall geolocation performance was assessed to be excellent. Although one of the images of the Rosamond site showed geolocation errors of approximately 10 m in range and 11 m in azimuth direction, exceeding the expected errors in both directions. Most of the imagery showed errors within the previously reported absolute location error range of 4 meters. The geolocation errors found at the other two test sites were measured to be within an average of 1.5 meters.

5 References

- Avci, K. & Nacaroglu, A., (2008). A New Window Based on Exponential Function, in *2008 Ph. D. Research in Microelectronics and Electronics*, IEEE, 2008, pp. 69–72.
- Capella Space, (2022). Capella Space SAR Imagery Products Guide, v3.4. <https://support.capellaspace.com/hc/en-us/articles/4626115099796-SAR-Imagery-Products-Guide>
- Capella Space, (2023). Capella Space SAR Products Format Specification, v1.4. <https://support.capellaspace.com/hc/en-us/articles/5607458273940-SAR-Imagery-Products-Format-Specification>
- ESA (2022). EDAP Technical Note for Capella Data Assessment, v1.0. July 3, 2022. <https://earth.esa.int/eogateway/documents/20142/37627/Technical%20Note%20for%20Capella%20Data%20Assessment.pdf>.
- ESA-NASA, (2024). Joint Earth Observation Mission Quality Assessment Framework – SAR Guidelines, Rev-002.
- Gelaro, R., McCarty, W., Suárez, M. J., Todling, R., Molod, A., Takacs, L., Randles, C. A., Darmenov, A., Bosilovich, M. G., Reichle, R., & others. (2017). The modern-era retrospective analysis for research and applications, version 2 (MERRA-2). *Journal of Climate*, 30(14), 5419–5454.
- JCGM, (2008). ‘Evaluation of measurement data - Guide to the expression of uncertainty in measurement’, JCGM, 100. Available at: https://www.bipm.org/utils/common/documents/jcgm/JCGM_100_2008_E.pdf (Accessed: ???).
- Li, X.-M., & Lehner, S. (2013). Algorithm for sea surface wind retrieval from TerraSAR-X and TanDEM-X data. *IEEE Transactions on Geoscience and Remote Sensing*, 52(5), 2928–2939.
- Marinkovic, P., Ketelaar, G., van Leijen, F., & Hanssen, R. (2007). InSAR quality control: Analysis of five years of corner reflector time series. Proceedings of the Fringe 2007 Workshop (ESA SP-649), Frascati, Italy, 26–30.
- Ulaby, F., Dobson, M. C., & Álvarez-Pérez, J. L. (2019). *Handbook of radar scattering statistics for terrain*. Artech House.

APPENDIX A

Table A1. Capella Space data products used for the assessment.

Test Area	Satellite Number	Imaging Mode	Polarization	Acquisition Date	Incidence Angle	Software version
Rosamond, California	C03	SM	VV	20220530	29.7	2.24.0
	C03	SM	VV	20220626	40.2	2.25.4
	C05	SM	VV	20220811	44.2	2.27.1
	C07	SM	VV	20220507	37.9	2.22.3
	C07	SM	VV	20220610	40.3	2.24.3
	C07	SM	VV	20220617	40.2	2.25.1
	C07	SM	VV	20220803	46.1	2.27.0
	C07	SM	VV	20220907	47.9	2.28.3
	C07	SM	VV	20221013	35.8	2.30.2
	C07	SM	VV	20221022	42.5	2.31.1
	C07	SM	VV	20221221	47.3	2.33.3
	C07	SM	VV	20230405	42.1	2.38.5
	C08	SM	VV	20220327	40.7	2.21.1
	C08	SM	VV	20220410	33.1	2.21.2
	C08	SM	VV	20220521	36.3	2.24.0
	C08	SM	VV	20220724	36.4	2.26.1
	C08	SM	VV	20221031	28.4	2.31.1
	C08	SM	VV	20221108	34.4	2.31.2
C08	SM	VV	20230120	43.4	2.34.0	
C08	SM	VV	20230317	38.7	2.38.4	
Doldrums	C10	SM	HH	20240517	50.7	2.57.3
	C09	SM	HH	20240518	30.5	2.57.3
	C14	SM	HH	20240519	23.3	2.57.3
	C10	SM	HH	20240522	45.9	2.57.4
	C09	SM	HH	20240523	46.3	2.57.4
	C09	SM	HH	20240529	39.8	2.57.4
	C10	SM	HH	20240601	39.6	2.57.4
	C09	SM	HH	20240609	53.7	2.57.4
	C14	SS	VV	20240525	38.3	2.57.4
	C09	SS	VV	20240525	24.2	2.57.4
C09	SS	HH	20240527	45.9	2.57.4	
C10	SS	HH	20240530	35.1	2.57.4	
Amazon	C10	SM	HH	20240520	50.9	2.57.3
	C09	SM	HH	20240521	41.7	2.57.3
	C10	SM	VV	20240523	49.3	2.57.4
	C10	SM	VV	20240523	44.1	2.57.4
	C09	SM	VV	20240524	54.0	2.57.4
	C09	SM	VV	20240524	47.7	2.57.4
	C10	SM	HH	20240524	46.9	2.57.4
	C10	SM	VV	20240525	26.8	2.57.4
	C09	SM	HH	20240525	54.9	2.57.4
	C10	SM	VV	20240526	54.3	2.57.4
	C09	SM	VV	20240526	17.2	2.57.4
	C09	SM	VV	20240527	39.0	2.57.4
C09	SM	VV	20240527	45.8	2.57.4	
C10	SM	VV	20240528	40.5	2.57.4	

lite Data Acquisition Program

Capella Space Radiometric and Geometric Quality Assessment Report

Test Area	Satellite Number	Imaging Mode	Polarization	Acquisition Date	Incidence Angle	Software version
	C10	SM	HH	20240529	43.7	2.57.4
	C09	SM	HH	20240601	25.0	2.57.4
	C14	SS	VV	20240524	28.0	2.57.4
	C10	SS	VV	20240525	48.0	2.57.4
	C09	SS	HH	20240526	28.2	2.57.4
	C14	SS	VV	20240527	28.0	2.57.4
	C09	SS	VV	20240527	37.2	2.57.4
	C14	SS	VV	20240530	28.0	2.57.4
	C10	SS	VV	20240530	45.3	2.57.4
	C09	SS	HH	20240601	19.9	2.57.4
	C09	SS	VV	20240601	53.2	2.57.4
	C09	SS	VV	20240602	30.7	2.57.4
	C10	SS	HH	20240603	37.6	2.57.4
	C10	SS	VV	20240604	43.5	2.57.4
	C09	SS	HH	20240606	43.6	2.57.4
	C10	SS	HH	20240608	36.7	2.57.4
	C09	SS	VV	20240608	26.4	2.57.4

Table A2. List of Capella acquisitions used for the IRF assessment.

Test Area	Satellite Number	Imaging Mode	Polarization	Acquisition Date	Incidence Angle	Software version
Rosamond, California	C02	SM	HH	20210727	37.71	2.52.0
	C03	SM	HH	20210625	30.30	2.6.0
	C03	SM	VV	20220530	29.72	2.24.0
	C03	SM	VV	20220626	40.23	2.25.4
	C03	SM	HH	20220818	38.92	2.27.1
	C05	SM	VV	20220402	32.11	2.21.2
	C05	SM	HH	20220709	32.21	2.26.1
	C05	SM	VV	20220811	44.22	2.27.1
	C05	SM	HH	20221214	45.38	2.33.3
	C07	SM	HH	20220327	44.56	2.21.1
	C07	SM	VV	20220507	37.88	2.22.3
	C07	SM	VV	20220610	40.31	2.24.3
	C07	SM	VV	20220617	40.16	2.25.1
	C07	SM	VV	20220803	46.07	2.27.0
	C07	SM	VV	20220907	47.87	2.28.3
	C07	SM	VV	20221013	35.83	2.30.2
	C07	SM	VV	20221022	42.49	2.31.1
	C07	SM	VV	20221221	47.26	2.33.3
	C07	SM	VV	20230310	32.76	2.38.3
	C07	SM	VV	20230405	42.08	2.38.5
	C08	SM	HH	20220319	26.76	2.19.2
	C08	SM	VV	20220327	40.75	2.21.1
	C08	SM	VV	20220410	33.08	2.21.2
C08	SM	VV	20220521	36.32	2.24.0	
C08	SM	VV	20220724	36.40	2.26.1	

lite Data Acquisition Program

Capella Space Radiometric and Geometric Quality Assessment Report

Test Area	Satellite Number	Imaging Mode	Polarization	Acquisition Date	Incidence Angle	Software version
	C08	SM	VV	20221031	28.41	2.31.1
	C08	SM	VV	20221108	34.36	2.31.2
	C08	SM	HH	20221218	40.22	2.34.0
	C08	SM	VV	20230120	43.38	2.34.0
	C08	SM	VV	20230317	38.73	2.38.4
	C09	SM	HH	20240205	43.19	2.53.1
	C09	SM	HH	20240218	43.00	2.54.0
	C10	SM	HH	20240315	46.22	2.56.0
	C03	SP	HH	20210603	29.11	2.8.0
	C03	SP	HH	20210917	38.31	2.8.1
	C05	SP	HH	20221206	29.14	2.33.3
	C07	SP	HH	20230609	37.77	2.42.1
	C08	SP	HH	20221231	36.13	2.53.1
	C09	SS	HH	20240523	52.09	2.57.4
	C09	SS	HH	20240526	54.65	2.57.4
	C09	SS	HH	20240527	24.60	2.57.4
	C09	SS	HH	20240528	42.68	2.57.4
	C09	SS	HH	20240601	51.69	2.57.4
	C10	SS	HH	20240525	48.52	2.57.4
	C10	SS	HH	20240527	53.70	2.57.4
	C10	SS	HH	20240530	16.91	2.57.4
	C10	SS	HH	20240530	46.63	2.57.4
	C10	SS	HH	20240604	45.26	2.57.4
	C14	SS	HH	20240523	55.43	2.57.4
	C14	SS	HH	20240524	17.15	2.57.4
	C14	SS	HH	20240525	50.55	2.57.4
	C14	SS	HH	20240526	55.49	2.57.4
	C14	SS	HH	20240527	17.14	2.57.4
	C14	SS	HH	20240529	55.46	2.57.4
	C14	SS	VV	20240530	17.17	2.57.4
	C14	SS	HH	20240531	50.57	2.57.4
	C14	SS	HH	20240601	55.43	2.57.4
	C14	SS	HH	20240604	55.44	2.57.4
	C14	SS	VV	20240605	17.15	2.57.4
Oklahoma	C09	SM	HH	20240518	54.739	2.57.3
	C09	SM	HH	20240526	21.181	2.57.4
	C09	SM	HH	20240528	46.378	2.57.4
	C10	SM	HH	20240525	28.359	2.57.4
	C14	SM	HH	20240515	51.358	2.57.3
	C14	SM	HH	20240518	48.577	2.57.3
	C14	SM	HH	20240523	19.965	2.57.4
	C14	SM	HH	20240525	58.162	2.57.4
	C14	SM	HH	20240527	45.385	2.57.4
	C14	SM	HH	20240528	58.164	2.57.4

lite Data Acquisition Program

Capella Space Radiometric and Geometric Quality Assessment Report

Test Area	Satellite Number	Imaging Mode	Polarization	Acquisition Date	Incidence Angle	Software version
	C09	SS	HH	20240601	25.602	2.57.4
	C09	SS	HH	20240603	48.310	2.57.4
	C09	SS	HH	20240607	40.682	2.57.4
	C10	SS	HH	20240531	44.019	2.57.4
	C10	SS	HH	20240601	52.670	2.57.4
	C10	SS	HH	20240604	31.876	2.57.4
	C14	SS	HH	20240529	19.660	2.57.4
	C14	SS	HH	20240601	19.713	2.57.4
	C14	SS	HH	20240602	45.420	2.57.4
	C14	SS	HH	20240604	19.702	2.57.4
OPERA site, California	C09	SM	VV	20240602	53.815	2.57.4
	C09	SM	VV	20240603	39.188	2.57.4
	C09	SM	VV	20240604	23.338	2.57.4
	C09	SM	HH	20240607	51.981	2.57.4
	C10	SM	VV	20240531	45.429	2.57.4
	C10	SM	HH	20240605	44.254	2.57.4
	C10	SM	HH	20240606	24.893	2.57.4
	C14	SM	HH	20240527	45.699	2.57.4
	C14	SM	VV	20240530	45.507	2.57.4
	C14	SM	VV	20240602	45.638	2.57.4
	C14	SM	HH	20240605	45.697	2.57.4
	C14	SM	HH	20240608	45.497	2.57.4
	C09	SS	HH	20240523	33.012	2.57.4
	C09	SS	HH	20240529	53.870	2.57.4
	C09	SS	HH	20240602	29.051	2.57.4
	C10	SS	HH	20240526	47.173	2.57.4
	C10	SS	HH	20240601	28.195	2.57.4
	C10	SS	HH	20240601	54.512	2.57.4